The Use of Conductivity Measurements for the Characterization of Cationic Palladium(II) Complexes and for the Determination of Kinetic and Thermodynamic Data in Palladium-Catalyzed Reactions

Anny Jutand[a]

Keywords: Cationic complex / Conductivity / Kinetics / Mechanism / Palladium

This review illustrates how conductivity measurements are used to characterize the *cationic* character of aryl-, vinyl-, hydrido-, and (η^3-allyl)palladium(II) complexes generated by oxidative addition of aryl and vinyl triflates, acetic/formic acid, and allylic carboxylates/carbonates, respectively, with palladium(0) complexes in DMF. These cationic palladium(II) complexes have been postulated as key intermediates in Stille, Heck, Tsuji–Trost, and Trost reactions, but most of them have never been characterized in the context of real oxidative additions, i.e., with the counteranion delivered by the reagent (triflates, carboxylates, and carbonates). The role of chloride ions has been examined and the mechanistic consequences are reported. Conductivity measurements are also used to obtain thermodynamic and kinetic data on the formation of cationic palladium(II) complexes and, consequently, to gain a deeper insight into the mechanism of palladium-catalyzed reactions. The *reversibility* of oxidative additions of acetic/formic acid and allylic carboxylates/carbonates with Pd^0 complexes has been established and equilibrium constants have been determined. The isomerization of cyclic *trans*/*cis* cationic (η^3-allyl)palladium(II) complexes is evidenced by a rate constant that depends on the Pd^0 precursor: kinetic evidence for an S_N2 mechanism that is responsible for the loss of stereoselectivity observed in catalytic reactions. Under conditions in which the oxidative additions are irreversible, the *kinetics* of the formation of cationic (η^3-allyl)palladium(II) complexes has been monitored by conductivity measurements for the determination of the rate constants. By comparing the rate of disappearance of Pd^0, it has been shown that oxidative additions of allylic carboxylates proceed in two steps with the detection of intermediate neutral, kinetic Pd^0 complexes ligated to the allylic carboxylate unit. As an example of its application, the mechanism of a Stille reaction has been investigated by conductivity measurements of an ionic by-product in DMF.

Introduction

Many palladium-catalyzed reactions involve cationic palladium(II) complexes generated in the first step of the catalytic cycle. In Heck reactions[1] with aryl triflates (ArOTf, Tf = SO_2CF_3),[1,2] [Equation (1)], cationic arylpalladium(II) complexes are formed in the oxidative addition of aryl triflates to Pd^0 complexes [Equation (2), L = monodentate ligand or L_2 = bidentate ligand].

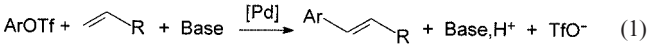

(1)

(2)

In Tsuji−Trost reactions [Equation (3)], cationic (η^3-allyl)palladium(II) complexes are formed in the oxidative addition of allylic carboxylates (or carbonates) to Pd^0 complexes [Equation (4)].[3]

[a] Ecole Normale Supérieure, Département de Chimie, UMR CNRS 8640,
24, Rue Lhomond, 75231 Paris Cedex 5, France
Fax: (internat.) + 33-1/44323325
E-mail: Anny.Jutand@ens.fr

Anny Jutand was born in France in 1948. She studied chemistry at the Ecole Nationale Supérieure de Chimie de Paris (MS degree, University Paris VI, 1971). She obtained her Doctorate under the direction of Professor J. F. Fauvarque at the University Paris XIII in Villetanneuse. After a postdoctoral stay with Professor B. Åkermark at the Royal Institute of Technology in Stockholm, she moved back to the University Paris XIII. In 1984, she joined Dr. C. Amatore's group at the Ecole Normale Supérieure in Paris. She became Research Director at CNRS (a position equivalent to a full Professor) in 1992. Her current research interests are centered on the investigation of the mechanism of transition metal catalyzed reactions and the development of reactions that require activation by both a transition metal and electron transfer.

MICROREVIEWS: This feature introduces the readers to the authors' research through a concise overview of the selected topic. Reference to important work from others in the field is included.

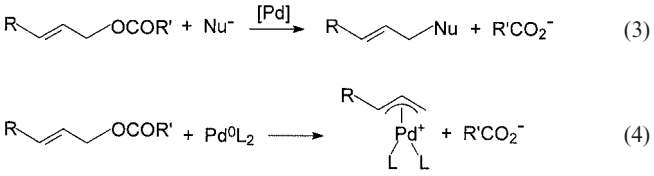

Most cationic complexes postulated, however, as key intermediates have not been characterized under the conditions of real oxidative additions. This review illustrates how, by using conductivity measurements,[4,5] cationic palladium(II) complexes formed in oxidative additions may be detected and characterized[6] under the real conditions of a catalytic reaction. Moreover, since the conductivity of free ionic species is proportional to their concentration,[5] this technique can also be used to obtain thermodynamic and kinetic data for the formation of cationic palladium(II) complexes and, consequently, to obtain a deeper insight into the mechanism of palladium-catalyzed reactions.

I. Observation by Conductivity Measurements of Cationic Arylpalladium(II) Complexes in the Oxidative Addition of Aryl Triflates to Neutral Pd^0 Complexes

Since 1984, aryl (or vinyl) triflates often have been used, instead of aryl (or vinyl) halides, in palladium-catalyzed Heck reactions [Equation (1)][2] or Stille reactions [Equation (5)].[7]

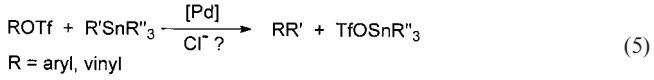

Such reactions, however, are greatly affected by the presence of chloride ions, which are added in large excess relative to the palladium catalyst. Extra chloride ions are always required in the case of Stille reactions involving vinyl triflates [Equation (5)].[7a,7b] A mechanistic investigation of the oxidative addition of vinyl triflates to $Pd^0(PPh_3)_4$, reported by Scott and Stille in 1986,[7b] revealed that undefined unstable complexes were formed in THF, whereas stable, well-characterized neutral $(\eta^1\text{-vinyl})Pd^{II}Cl(PPh_3)_2$ complexes were generated when the oxidative addition was performed in the presence of chloride ions. The undefined complexes were postulated to be unstable cationic complexes $[(\eta^1\text{-vinyl})Pd^{II}(PPh_3)_n]^+TfO^-$ (n = 2 or 3). In 1989, Stang et al. established that well-characterized cationic complexes $[(\eta^1\text{-vinyl})Pt^{II}(PPh_3)_3]^+TfO^-$ are formed in the oxidative addition of vinyl triflates to $Pt^0(PPh_3)_4$ in toluene.[8]

To explain the effect of chloride ions on the efficiency of palladium-catalyzed Stille reactions involving aryl triflates, Echavarren and Stille[7c] proposed in 1987 that neutral complexes $ArPdCl(PPh_3)_2$ were produced when the oxidative addition of $Pd^0(PPh_3)_4$ was performed in the presence of chloride ions, whereas decomposition took place in the absence of chloride ions. To characterize cationic complexes $[ArPd(PPh_3)_n]^+$ that would be formed in the oxidative addition of aryl triflates to $Pd^0(PPh_3)_4$, the reaction was reinvestigated by Farina et al. in 1993 in the polar solvent NMP. The authors could not conclude, however, what the structure is of the arylpalladium(II) complex formed in the absence of chloride ions in NMP.[9]

Until 1995, none of the complexes $[ArPdL_n]^+TfO^-$ or $[(\eta^1\text{-vinyl})PdL_n]^+TfO^-$ had been characterized in the oxidative addition of aryl or vinyl triflates, respectively, to Pd^0 complexes.

I.1 Evidence from Conductivity Measurements for the Formation of Cationic *trans*-$[ArPdL_2S]^+$ Complexes in the Oxidative Addition of Aryl Triflates to Neutral Pd^0 Complexes in DMF

In 1995, the cationic character of $[ArPd^{II}(PPh_3)_2S]^+$ complexes, formed in the oxidative addition of aryl triflates to a halide-free Pd^0 complex such as $Pd^0(PPh_3)_4$, was established by conductivity measurements in DMF [Equation (6), L = PPh_3, S = solvent].[10]

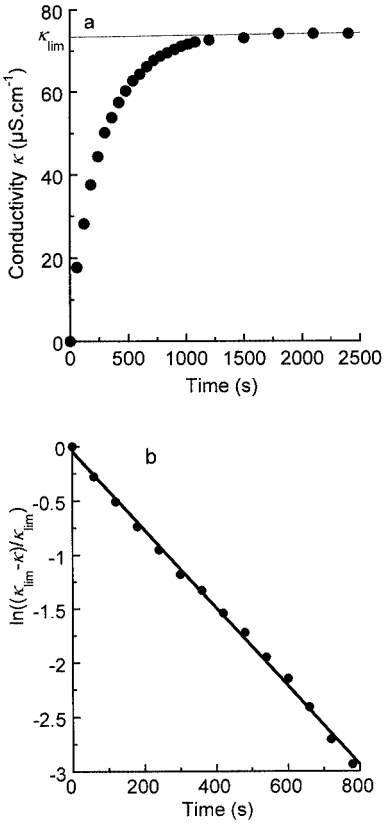

Figure 1. Kinetics of the formation of *trans*-[4-$O_2NC_6H_4Pd(PPh_3)_2(DMF)]^+TfO^-$ in the oxidative addition of 4-$O_2NC_6H_4OTf$ (10 mM) to $Pd^0(PPh_3)_4$ (2 mM) in DMF at 20 °C: (a) variation of the conductivity versus time; $\kappa = \kappa_{exp} - \kappa_0$ (κ_{exp}: experimental conductivity at t; κ_0: initial residual conductivity of 2 $\mu S \cdot cm^{-1}$); (b) variation of $\ln[(\kappa_{lim} - \kappa)/\kappa_{lim})]$ versus time; κ: conductivity at t; κ_{lim}: final conductivity

$$ArOTf + Pd^0L_4 \xrightarrow{k_{app}} ArPdL_2S^+ + TfO^- + 2\,L \quad (6)$$

Indeed as is shown in Figure 1 (a), the conductivity (κ) of a solution of $Pd^0(PPh_3)_4$ (2 mM) in DMF (residual conductivity: $\kappa_0 = 2\ \mu S{\cdot}cm^{-1}$) increased upon addition of an aryl triflate (4-$O_2NC_6H_4OTf$) to reach a final, constant conductivity, κ_{lim}. This limiting value was obtained after the oxidative addition was complete, as confirmed by the total disappearance of $Pd^0(PPh_3)_4$, monitored simultaneously by amperometry.[10] This experiment shows that ionic species are formed in the oxidative addition. Moreover, such ionic species are rather stable, as is attested by the observed constant limiting value, κ_{lim} (Figure 1, a).

Cationic complexes were then isolated after an oxidative addition performed in a toluene/DMF solution. Analyses by FAB and electrospray mass spectrometry delivered values of *m*/*z* corresponding to the $[ArPd(PPh_3)_2]^+$ cations (Ar = 4-ClC_6H_4 and 4-$O_2NC_6H_4$) with the predicted isotope pattern expected for the Pd atom. The TfO^- anion was also characterized by FAB spectrometry.[10] Additionally, these complexes were characterized by ^{31}P NMR spectroscopy performed in DMF. The observation of one singlet in the ^{31}P NMR spectrum, even in the presence of excess PPh_3 released from $Pd^0(PPh_3)_4$ [Equation (6)], establishes that the cationic complex contains only two phosphane ligands. Moreover, those two phosphane ligands sit in a relative *trans* orientation on the Pd^{II} atom, with the fourth position being occupied by the solvent as in compound **1**.[10] Consequently, the cationic complexes $[ArPd(PPh_3)_3]^+TfO^-$ are not generated in DMF.

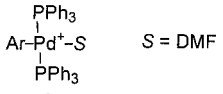

1

The association of the cations *trans*-$[ArPdL_2S]^+$ with the anion TfO^- was studied by observing the variation of their conductivities versus their concentration. In DMF, the conductivity of the ionic species, determined by the value of κ_{lim} (as in Figure 1, a), varied linearly with the palladium concentration in the range $0.5-3 \times 10^{-3}$ M (Figure 2, a).[10] This study established that free ions, *trans*-$[ArPdL_2(DMF)]^+$ and TfO^-, are formed in DMF [Equation (7), L = PPh_3].

$$ArOTf + Pd^0L_4 \xrightarrow{DMF} \underset{trans}{ArPdL_2(DMF)^+} + TfO^- + 2\,L \quad (7)$$

The molar conductivity Λ_M of these ions was calculated in DMF at 20 °C. The values are indicative of 1:1 electrolytes in solution in DMF:[6]

$\Lambda_M = 35\ (\pm 2)\ S{\cdot}cm^2{\cdot}mol^{-1}$ for *trans*-$[4\text{-}O_2NC_6H_4Pd(PPh_3)_2(DMF)]^+TfO^-$

$\Lambda_M = 57\ (\pm 2)\ S{\cdot}cm^2{\cdot}mol^{-1}$ for *trans*-$[4\text{-}ClC_6H_4Pd(PPh_3)_2(DMF)]^+TfO^-$

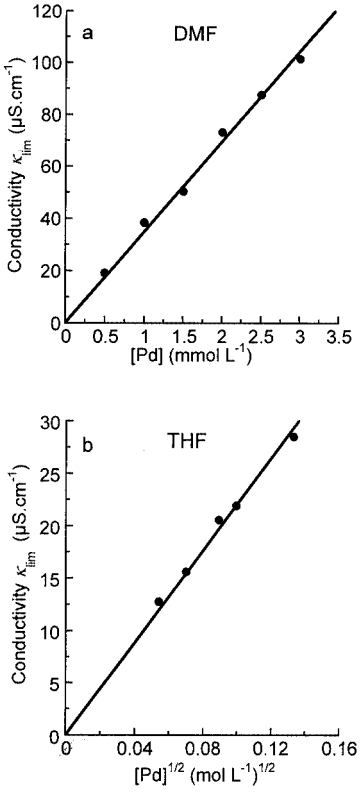

Figure 2. (a) Variation of the conductivity of *trans*-$[4\text{-}O_2NC_6H_4Pd(PPh_3)_2(DMF)]^+TfO^-$ in DMF, determined by the value of κ_{lim} (Figure 1, a) versus the concentration of Pd initially introduced as $Pd^0(PPh_3)_4$ before reaction with 4-$O_2NC_6H_4OTf$, at 20 °C; (b) variation of the conductivity of *trans*-$[4\text{-}O_2NC_6H_4Pd(PPh_3)_2(THF)]^+TfO^-$ in THF (determined as in Figure 2, a) versus the square root of the Pd concentration, at 20 °C

In THF, the conductivity of the ionic species formed in the oxidative addition was lower than that observed in DMF. Moreover, the conductivity varied linearly with the square root of the palladium concentration (Figure 2, b).[10] This observation establishes that free ions *trans*-$[ArPd(PPh_3)_2(THF)]^+$ and TfO^- are formed in THF,[11] but they are involved in an equilibrium with the neutral complex $[ArPd(OTf)(PPh_3)_2]$.[13]

The effect of additives (chloride or acetate ions) on the structure of the cationic complexes has been tested. Addition of chloride ions, from nBu_4NCl (2 mM), to a solution of *trans*-$[4\text{-}O_2NC_6H_4Pd(PPh_3)_2(DMF)]^+TfO^-$ (2 mM) in DMF resulted in a conductivity lower than the sum of the intrinsic conductivities of *trans*-$[4\text{-}O_2NC_6H_4\text{-}Pd(PPh_3)_2(DMF)]^+TfO^-$ and $nBu_4N^+Cl^-$.[10] This observation is indicative of the formation of a neutral complex, which was identified as *trans*-4-$O_2NC_6H_4PdCl(PPh_3)_2$ [Equation (8), L = PPh_3] by comparison with an authentic sample.

$$ArPdL_2(DMF)^+ + TfO^- + nBu_4N^+ + Cl^- \longrightarrow ArPdClL_2 + TfO^- + nBu_4N^+ \quad (8)$$

It has also been observed that the oxidative addition in DMF of aryl triflates to the anionic Pd^0 complex $[Pd^0(PPh_3)_2Cl]^-$, generated by addition of chloride ions to $Pd^0(PPh_3)_4$ or by the electrochemical reduction of $PdCl_2(PPh_3)_2$,[14] gave the neutral *trans*-$ArPdCl(PPh_3)_2$ (Scheme 1).[10,15]

Scheme 1. Oxidative addition of aryl triflates to anionic Pd^0 complexes

Similarly, the oxidative addition in DMF of aryl triflates to the anionic Pd^0 complex $[Pd^0(PPh_3)_2(OAc)]^-$, generated from $Pd(OAc)_2$ and 3 equiv. of PPh_3,[16] led to neutral complexes *trans*-$ArPd(OAc)(PPh_3)_2$ (Scheme 2).[15] At low concentrations, some *trans*-$[ArPd(PPh_3)_2(DMF)]^+$ may still coexist with *trans*-$ArPd(OAc)(PPh_3)_2$ since the partial dissociation of the latter to the cationic complex and AcO^- has been established independently ($K_{diss} = 1.3 \times 10^{-3}$ M).[16b,16c]

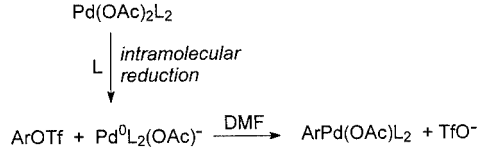

Scheme 2. Oxidative addition of aryl triflates to anionic Pd^0 complexes

Consequently, in the case of the *monodentate phosphane* PPh_3, cationic complexes *trans*-$[ArPdL_2(DMF)]^+$ (TfO^- counteranion) are generated in the oxidative addition of aryl triflates to neutral Pd^0 complexes in DMF, whereas neutral complexes *trans*-$[ArPdXL_2]$ (X = Cl, OAc) are formed in the oxidative addition to anionic Pd^0 complexes ligated by chloride or acetate ions.

The oxidative addition of aryl triflates to Pd^0 complexes ligated to *bidentate bis(phosphane)* (P,P) ligands has also been investigated. When the oxidative addition of aryl triflates [Ar = 4-$O_2NC_6H_4$, 3,5-$(CF_3)_2C_6H_3$, C_6H_5] to $Pd^0(dppf)(\eta^2\text{-}CH_2{=}CHCO_2Me)$ was performed in THF, the resulting cationic $[ArPd(dppf)(THF)]^+$ complexes were not stable at room temperature.[17] Stable, neutral ArPdCl(dppf), ArPdI(dppf) and ArPd(OAc)(dppf) complexes were obtained, however, when the oxidative additions were performed in the presence of chloride, iodide or acetate ions, respectively.[17] Recently, Alcazar–Roman and Hartwig reported data on the oxidative addition of phenyl triflate to $Pd^0(BINAP)_2$ in THF. A stable cationic complex was obtained only in the presence of an amine: $[PhPd(BINAP)(NH_2R)]^+TfO^-$ (R = alkyl).[18]

Oxidative additions, however, of aryl triflates to Pd^0 ligated to bis(phosphane) (P,P) ligands are sluggish reactions.[17–19] To bypass this problem, chemists interested in the mechanism of reactions involving cationic $[ArPd(P,P)S]^+TfO^-$ complexes (supposedly formed in the oxidative addition of aryl triflates) have synthesized such complexes by treating ArPdX(P,P) (X = I, Br, Cl) with AgOTf.[18–21] Using this strategy, Brown and Hii characterized complexes $[ArPd(dppf)(THF)]^+TfO^-$ [Ar = Ph, 4-$CH_3OC_6H_4$, 3,5-$(CF_3)_2C_6H_3$] in THF at low temperatures ($\leq$ 0 °C); they found that [{3,5-$(CF_3)_2C_6H_3$}Pd(dppf)(DMF)]$^+TfO^-$ is stable at room temperature in DMF.[20b] In a similar manner, Espinet et al. reported that stable complexes $[ArPd(dppe)(THF)]^+TfO^-$ (Ar = C_6F_5, $C_6Cl_2F_3$) can be synthesized in THF.[19] These complexes have been characterized by conductivity measurements.[19,20b] Ludwig et al. have synthesized complexes $[PhPd(P,P)(DMF)]^+TfO^-$ (P,P = dppe, dppp, dcpe), which are stable at 0 °C.[21]

Consequently, polar solvents such as DMF (and, to lesser extent, THF) and amines appear to be good coordinating solvents and ligands, respectively, for the stabilization of cationic complexes $[ArPdL_2S]^+TfO^-$ [L = monophosphane or L_2 = bis(phosphane), *S* = solvent or amine] formed in the oxidative addition of aryl triflates to neutral Pd^0 complexes.

I.2 Kinetics of the Formation of Cationic $[ArPd(PPh_3)_2S]^+$ Complexes in the Oxidative Addition of Aryl Triflates to Neutral Pd^0 Complexes in DMF Monitored by Conductivity Measurements – Influence of Chloride Ions

Any oxidative addition performed using $Pd^0(PPh_3)_4$ involves $SPd^0(PPh_3)_2$ [22] as the reactive complex generated from $Pd^0(PPh_3)_3$ [23] in an endergonic and fast equilibrium (Scheme 3).

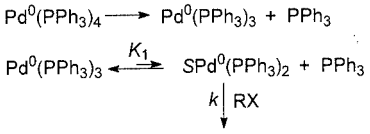

Scheme 3. Mechanism of oxidative additions from $Pd^0(PPh_3)_4$ (*S* = solvent)

The oxidative addition of aryl triflates with $Pd^0(PPh_3)_4$ [Equation (6)] is then an overall reaction that proceeds via $SPd^0(PPh_3)_2$ and k_{app} is the apparent rate constant of the overall reaction ($k_{app} = K_1k/[PPh_3]$).[22]

Since the conductivity κ of $[ArPd(PPh_3)_2(DMF)]^+TfO^-$ in DMF is proportional to its concentration, the evolution of the conductivity κ with time, as observed in Figure 1 (a), characterizes the kinetics of the formation the cationic complex $[ArPd(PPh_3)_2(DMF)]^+$ in the oxidative addition of ArOTf to $Pd^0(PPh_3)_4$. The variation of $\ln[(\kappa_{lim} - \kappa)/\kappa_{lim}]$ versus time was linear (Figure 1, b): $\ln[(\kappa_{lim} - \kappa)/\kappa_{lim}] = -k_{app}[ArOTf]t$.[10] The slope of the line gives the value of the rate constant for the formation of the cationic complex (0.35 ± 0.02 $M^{-1}s^{-1}$ for 4-$O_2NC_6H_4OTf$ in DMF at 20 °C). This rate constant is very similar to the rate constant of the disappearance of the Pd^0 complex monitored independently by amperometry ($k_{app} = 0.32 \pm 0.02$ $M^{-1}s^{-1}$).[10] This observation shows that, if the oxidative addition involves the

Table 1. Accelerating effect of chloride ions [added as nBu$_4$NCl to Pd^0(PPh$_3$)$_4$ prior to the addition of ArOTf] on the rate of the oxidative addition of aryl triflates to Pd^0(PPh$_3$)$_4$ (c_0 = 2 mM) in DMF at 20 °C (Scheme 4)

ArOTf	4-O$_2$NC$_6$H$_4$OTf		C$_6$H$_5$OTf		1-Naphthyl−OTf	
Cl$^-$ equiv./[Pd^0(PPh$_3$)$_4$]	0	150	0	150	0	150
k_{app}^{Cl} [M^{-1}·s^{-1}]	0.32	0.59	1.7×10^{-3}	33×10^{-3}	7.5×10^{-2}	43×10^{-2}

formation of an intermediate neutral complex, ArPd(OTf)L$_2$, then the ionization of this neutral complex in DMF to [ArPdL$_2$(DMF)]$^+$ and TfO$^-$ is faster than the oxidative addition step. Consequently, the affinity of the anion TfO$^-$ for the Pd^{II} in DMF is very low.

Since chloride ions play an important role in the efficiency of palladium-catalyzed reactions performed from aryl triflates,[7d−7f,9] it was of interest to investigate a possible kinetic effect of chloride ions in the oxidative addition of aryl triflates. This effect cannot be monitored by conductivity measurements because of the high conductivity of nBu$_4$NCl when added in relatively large amounts. This problem was solved by investigating the kinetics of the oxidative addition of aryl triflates by amperometry.[10,22] This technique allows monitoring of the decay of the Pd^0 concentration in the oxidative addition by recording the decay of its oxidation current (which is proportional to its concentration) versus time, after addition of the aryl triflate. As summarized in Table 1, the effect of chloride ions [added as nBu$_4$NCl to Pd^0(PPh$_3$)$_4$ prior to the addition of the aryl triflate] is to accelerate the rate of the oxidative addition,[10] as a consequence of the formation of anionic [Pd^0(PPh$_3$)$_2$Cl]$^-$ complexes.[14] Addition of a rather large amount of chloride ions, relative to Pd^0(PPh$_3$)$_4$, is required to observe a significant accelerating effect with highly reactive triflates. The effect is more pronounced when poorly reactive aryl triflates are considered (Table 1).

Consequently, the chloride ions play a dual role in the oxidative addition of aryl triflates to Pd^0(PPh$_3$)$_4$: (i) acceleration of the oxidative addition and (ii) formation of neutral *trans*-ArPdCl(PPh$_3$)$_2$ complexes (Scheme 4).[10]

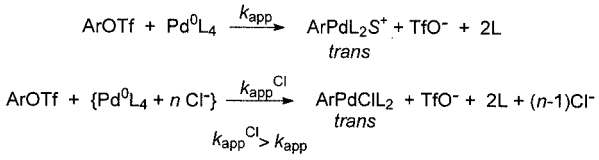

Scheme 4. Effect of chloride ions on the oxidative addition of aryl triflates to Pd^0(PPh$_3$)$_4$ in DMF

Since aryl triflates may supplant aryl halides in palladium-catalyzed reactions, it was of interest to compare their reactivity in oxidative additions to Pd^0(PPh$_3$)$_4$ (c_0 = 2 mM). The following order of reactivity in DMF was established: PhI >> PhOTf > PhBr >> PhCl, with rate constants at 20 °C of 17, 0.0017, and 0.001 M^{-1}s^{-1} for PhI, PhOTf and PhBr, respectively.[10] In DMF, the complexes *trans*-PhPdI(PPh$_3$)$_2$ and *trans*-PhPdBr(PPh$_3$)$_2$, formed by the oxidative additions of PhI and PhBr, respectively, partly dissociate to generate the cationic complexes *trans*-[PhPd(PPh$_3$)$_2$(DMF)]$^+$ [Equation (9), $K_I = 5.8 \times 10^{-4}$ M, $K_{Br} = 2.8 \times 10^{-4}$ M at 25 °C].[24] Since the values of the equilibrium constants K_I and K_{Br} are low, the degree of dissociation will be significant only at low concentrations.

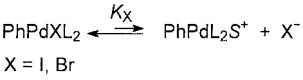

(9)

Conductivity measurements have also been used to characterize cationic complexes formed in the oxidative addition of aryl iodides to (P,N,P)Pd^0(dba) complexes in DMSO.[25] The ionic character found for complexes [ArPd(P,N,P)]$^+$ indicates that the (P,N,P) ligands behave as *tridentate* ligands for the Pd^{II} complex [Equation (10)]. The kinetics of formation of the cationic complexes has been monitored by conductivity measurements that have allowed determination of the rate constant k_{app} [Equation (10)].[25] The effect that the N-bearing substituent and the aryl group have on the rate of the oxidative addition was then investigated.

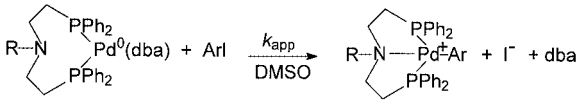

(10)

R= Ph, *t*Bu, 4-MeO-C$_6$H$_4$; Ar = Ph, 4-MeO-C$_6$H$_4$, 4-NO$_2$-C$_6$H$_4$

I.3 Conclusion and Mechanistic Consequences in Palladium-Catalyzed Stille and Heck Reactions: Cationic versus Neutral Arylpalladium(II) Complexes as Key Intermediates

On the basis of the kinetic data and the structures of arylpalladium complexes reported above, the mechanisms of palladium-catalyzed reactions involving aryl triflates (ArOTf) may differ from those involving aryl halides (ArX). On one hand, aryl triflates are less reactive than aryl iodides and so the oxidative addition (first step of the catalytic cycles) may become rate-determining when using aryl triflates. On the other hand, the formation of cationic *trans*-[ArPdL$_2$*S*]$^+$TfO$^-$ complexes from aryl triflates versus neutral *trans*-ArPdXL$_2$ from aryl halides may affect their reactions with nucleophiles: transmetallation with organostannanes in the case of Stille reactions [Equation (11)] and carbopalladation with alkenes in the case of Heck reactions [Equation (12)]. Moreover, the presence of chloride ions in reactions performed using aryl triflates[7a−7f,9,12] introduces

some complexity, since chloride ions accelerate the rate of the slow oxidative addition of aryl triflates and affect the structure of the arylpalladium(II) complex involved in the reaction with the nucleophile by formation of neutral *trans*-$ArPdClL_2$ complexes.

I.3.1 Stille Reactions

With regard to these observations, Espinet et al. have analyzed the puzzling role, positive or negative, depending on ligand and solvent, of chloride ions in Stille reactions involving aryl triflates (aryl = C_6F_5 or $C_6Cl_2F_3$) and CH_2=$CHSnBu_3$ [Equation (11)].[12]

$$ArOTf + RSnR'_3 \xrightarrow[Cl^- ?]{[Pd]} ArR + TfOSnR'_3 \quad (11)$$

In THF, whatever the ligand (PPh_3 or $AsPh_3$), neutral *trans*-$ArPdClL_2$ complexes are formed in the presence of chloride ions. When the palladium atom is ligated by $AsPh_3$, the transmetallation of CH_2=$CHSnBu_3$ with *trans*-$ArPdCl(AsPh_3)_2$ is fast and the oxidative addition of aryl triflates to $Pd^0(AsPh_3)_4$ is rate-determining. Thus, the positive role of chloride ions in this Stille reaction arises from an acceleration of the oxidative addition. When the palladium atom is ligated by PPh_3, the transmetallation with *trans*-$[ArPdCl(PPh_3)_2]$ becomes rate-determining. In this case, the inhibiting role of chloride ions in the Stille reaction arises from a deceleration of the transmetallation, which is even slower with neutral *trans*-$ArPdCl(PPh_3)_2$ complexes than with cationic complexes $[ArPdX'(PPh_3)_2]^+$ (X′ = PPh_3 or *S*) formed in the absence of chloride ions.[12]

I.3.2 Heck Reactions

The question of the reactivity of neutral versus cationic arylpalladium(II) complexes is also crucial in Heck reactions performed with aryl triflates [Equation (12)].[2]

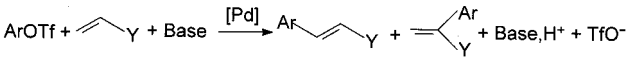

(12)

The simultaneous use of aryl triflates and *bidentate ligand* (P,P) may affect the reactivity, regioselectivity and enantioselectivity of the reactions. Indeed, the catalytic reactions work well with electron-rich alkenes (Y = OR, ...) and allow the unusual substitution by the aryl group at the more-substituted carbon atom of the alkene (α-arylation).[2] An "ionic" mechanism has been proposed by Cabri et al.[2a,2d,2f] and Hayashi et al.[2b,2c,2e] (Scheme 5). Cationic complexes $[ArPd(P,P)S]^+$ generated in the oxidative addition have a labile coordination site *cis* to the Ar group and easily react with electron-rich alkenes. The carbopalladation step (also called an insertion step) gives a cationic alkylPd^{II} complex in which the aryl group and the electron-donor group Y are attached to the same C atom (Scheme 5).

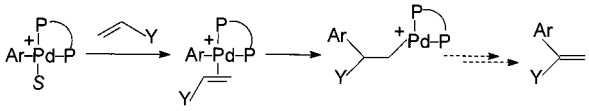

Scheme 5. Mechanism of the carbopalladation step from *cationic* arylpalladium(II) complexes ligated to bidentate (P,P) ligands

This mechanism will also operate with aryl halides, provided that silver[26a] or thallium[26b] salts are present to abstract the halide ion from ArPdX(P,P) to generate the cationic complexes $[ArPd(P,P)S]^+$.[20]

The mechanism of the formation of the arylated alkene from the intermediate cationic alkylPd^{II} complex[20b,27] is still under debate (Scheme 5). In the absence of a base, Brown and Hii have characterized by ^1H NMR spectroscopy the cationic alkylPd^{II} complex formed from $[PhPd(dppf)(THF)]^+$ and CH_2=$CHCO_2Me$ in THF at low temperatures (Scheme 6).[20b] The arylated alkene was formed by a β-hydride elimination (Scheme 6, path A). Neither $[HPd(P,P)S]^+$ nor $Pd^0(P,P)$ were detected, but a new cationic alkylPd^{II} species was observed to have formed by addition of the transient $[HPd(P,P)S]^+$ ion to the alkene CH_2=$CHCO_2Me$ (Scheme 6, path A). Consequently, no Pd^0 complex was generated from $[HPd(P,P)S]^+$ in the absence of a base. On the basis of DFT calculation, Deeth et al. have proposed the existence of a β-agostic hydrogen atom (Scheme 6, path B) because of the cationic character of the alkylpalladium(II) species formed in the carbopalladation step.[27a] Consequently, in the presence of a base, the Pd^0 complex would not be generated via a cationic palladium hydride formed by the traditional β-hydride elimination, but instead by deprotonation by the base of the acidic agostic proton (Scheme 6, path B).

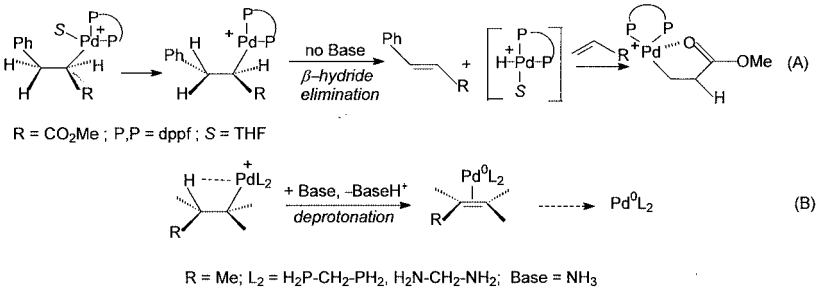

Scheme 6. Mechanism of the formation of an arylated alkene from *cationic* alkylpalladium(II) complexes ligated by bidentate ligands

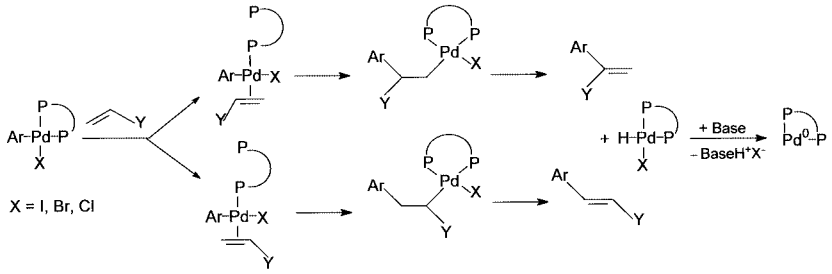

Scheme 7. Mechanism of the carbopalladation step from *neutral* arylpalladium(II) complexes ligated to bidentate (P,P) ligands, followed by β-hydride elimination and formation of a Pd^0 complex

A "neutral" mechanism is proposed when neutral ArPdX(P,P) complexes are generated in the oxidative addition of aryl halides (X = I, Br, Cl) or of aryl triflates in the presence of chloride ions (X = Cl).[2a,2d,2f] The neutral complexes would be less reactive than the cationic ones because the complexation of the alkene requires the unfavorable deligation of one P atom of the bis(phosphane) ligand. Moreover, such Heck reactions lead to nonselective α- and β-arylation (Scheme 7).[2a,2d,2f]

Although the "ionic" mechanism is supposed to induce better enantioselectivity in intramolecular Heck reactions,[2b,2c,2e,27b] Overman et al. have observed that the enantioselectivity is improved under the conditions of the "neutral" mechanism, i.e., from aryl iodides or from aryl triflates in the presence of chloride ions.[28] They propose the deligation of the halide as the key step responsible of this enantioselectivity, rather than deligation of one P atom of the bis(phosphane) via a pentacoordinate Pd^{II} transition state (Scheme 8).

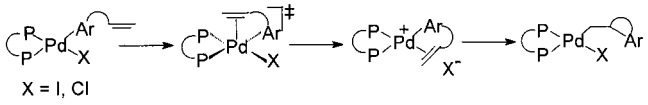

Scheme 8. Mechanism of the intramolecular carbopalladation step

As far as monodentate ligands (L) are concerned, cationic *trans*-$[ArPdL_2S]^+$ complexes appear to be more reactive than neutral *trans*-$ArPdXL_2$ (X = I) ones; they are, however, less reactive than *trans*-$ArPd(OAc)L_2$ complexes. The following order of reactivity with styrene has been observed in DMF:[16b,16c] *trans*-$PhPd(OAc)(PPh_3)_2$ > *trans*-$[PhPd(PPh_3)_2S]^+$ > *trans*-$PhPdI(PPh_3)_2$.

Because of the labile coordination site in the cationic complex *trans*-$[ArPdL_2S]^+$, no phosphane dissociation is required. The coordination of the alkene leads, however, to a *trans* complex, *trans*-$[ArPd(\eta^2\text{-alkene})L_2]^+$, which must reorganize to the *cis* complex (a thermodynamically unfavorable process) to allow alkene insertion into the Ar−Pd bond (Scheme 9). The evolution of the cationic alkylPd^{II} complex may then follow the mechanism proposed in Scheme 6 (path B) for bidentate ligands.

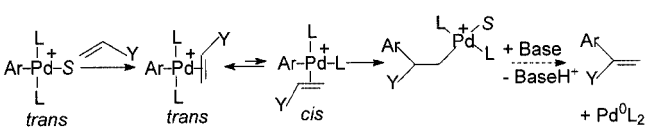

Scheme 9. Mechanism of the carbopalladation step from *cationic* arylpalladium(II) complexes ligated to monodentate ligands

The carbopalladation step from neutral *trans*-$ArPdXL_2$ complexes requires dissociation of one phosphane unit, which must be rate-determining when PPh_3 is considered (Scheme 10).

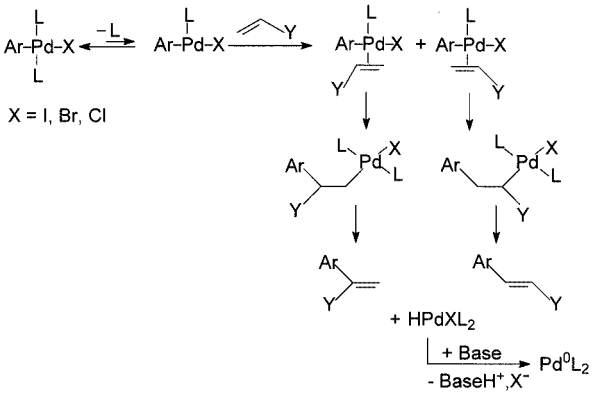

Scheme 10. Mechanism of the carbopalladation step from *neutral* arylpalladium(II) complexes ligated to monodentate ligands, followed by β-hydride elimination

When the Pd^0 precursor is $Pd(OAc)_2$ and PPh_3, *trans*-$ArPd(OAc)(PPh_3)_2$ complexes are generated in the oxidative addition of aryl triflates (Scheme 2)[15] or iodides.[16] The higher reactivity of *trans*-$ArPd(OAc)(PPh_3)_2$ compared to that of *trans*-$ArPdI(PPh_3)_2$ may be understood as a result of an easier displacement of the phosphane by the acetate, which may behave as a bidentate ligand[16c] {Scheme 11, see Sect. III for the existence of cationic $[HPdL_2(DMF)]^+$ formed in the β-hydride elimination step}.

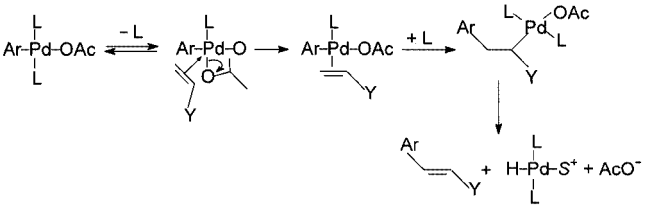

Scheme 11. Mechanism of the carbopalladation step from $ArPd(OAc)(PPh_3)_2$ complexes followed by β-hydride elimination in DMF

II. Formation of Cationic Palladium(II) Complexes in the Oxidative Addition of Vinyl Triflates or Benzoic Anhydride to $Pd^0(PPh_3)_4$ in DMF Observed by Conductivity Measurements

II.1 Formation of Cationic $[VinylPd(PPh_3)_2S]^+$ Complexes in the Oxidative Addition of Vinyl Triflates to Neutral Pd^0 Complexes in DMF Monitored by Conductivity Measurements

Since DMF appears to be a good coordinating solvent for cationic palladium(II) complexes, this property prompted us to investigate the mechanism of the oxidative addition of vinyl triflates to $[Pd^0(PPh_3)_4]$ in DMF. Cationic complexes *trans*-$[(\eta^1\text{-vinyl})Pd^{II}(PPh_3)_2(DMF)]^+TfO^-$ were generated and characterized by conductivity measurements (Figure 3), NMR spectroscopy, and electrospray mass spectrometry [Equation (13)].[29]

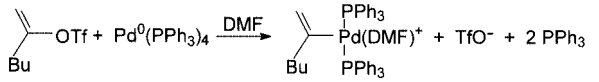

(13)

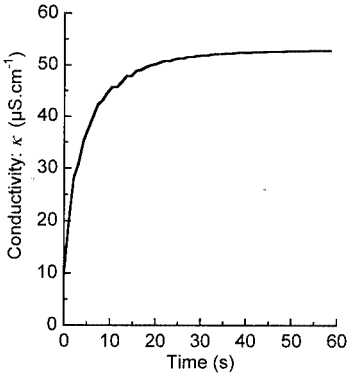

Figure 3. Kinetics of the formation of $[CH_2{=}C(n\text{Bu})Pd(PPh_3)_2(DMF)]^+TfO^-$ in the oxidative addition of $CH_2{=}C(n\text{Bu})OTf$ (2 mM) to $[Pd^0(PPh_3)_4]$ (2 mM) in DMF at 10 °C; variation of the conductivity κ versus time; $\kappa = \kappa_{exp} - \kappa_0$ (κ_{exp}: experimental conductivity at t; κ_0: initial residual conductivity of 3 $\mu S{\cdot}cm^{-1}$)

The oxidative addition was considerably faster than that of aryl triflates. Cationic vinylic complexes, however, were less stable than *trans*-$[ArPd(PPh_3)_2(DMF)]^+TfO^-$ since a slow degradation took place that gave the phosphonium salt $[vinylPPh_3]^+TfO^-$ together with a Pd^0 complex that was detected when the oxidative addition was performed under stoichiometric conditions [Equation (14)].[29]

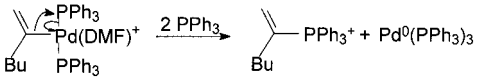

(14)

To date, in the vinylic series, the only stable cationic complexes characterized by conductivity measurements in CH_3NO_2 have been $[(\eta^1\text{-vinyl})Pt(PPh_3)_3]^+TfO^-$ formed in the oxidative addition of vinyl triflates to $Pt^0(PPh_3)_4$ in toluene, as reported by Stang et al.,[8] in which, in the absence of any coordinating solvent, a phosphane ligand occupies the fourth coordination site on the Pd^{II} center.

II.2 Formation of Cationic $[AcylPd(PPh_3)_2S]^+$ Complexes in the Oxidative Addition of Benzoic Anhydride to Neutral Pd^0 Complexes Monitored by Conductivity Measurements in DMF

Aromatic carboxylic anhydrides $(ArCO)_2O$ were introduced by Sakamoto et al. as *acylating* agents in palladium-catalyzed cross-coupling reactions (m = ZnX),[30a] and they have been used recently by Yamamoto et al. in Susuki-type reactions [m = $B(OH)_2$] [Equation (15)].[30b]

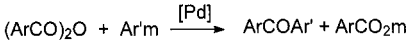

(15)

Recently, these compounds were used by de Vries et al. as *arylating* agents in palladium-catalyzed Heck reactions [Equation (16)].[31]

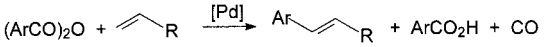

(16)

The mechanism of the oxidative addition of the benzoic anhydride to $Pd^0(PPh_3)_4$ (2 mM) has been investigated in DMF. Two $acylPd^{II}$ complexes have been identified (Scheme 12). The cationic complex *trans*-$[(PhCO)Pd(PPh_3)_2(DMF)]^+$, with $PhCO_2^-$ as the counteranion, was detected by conductivity measurements.[32]

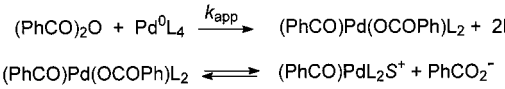

Scheme 12. Oxidative addition of benzoic anhydride to $Pd^0(PPh_3)_4$ in DMF ($k_{app} = 3 \times 10^{-3}\ M^{-1}s^{-1}$)

The neutral and cationic $acylPd^{II}$ complexes did not undergo any decarbonylation, which would have generated $phenylPd^{II}$ complex(es), a process required in the Heck reaction [Equation (16)]. Exchanging the two monodentate PPh_3 units with one bidentate ligand, dppp, gave a mixture of $[(PhCO)Pd(dppp)(DMF)]^+PhCO_2^-$ and (PhCO)Pd(OCOPh)(dppp) without any detectable decarbonylation process occurring.[32] Consequently, this reaction excludes the use of phosphane ligands in Heck reactions performed with $(PhCO)_2O$ that are, indeed, efficient with Pd^0 precursors consisting of Pd^{II} salts in the absence of any phosphane ligand.[31]

III. Reversible Formation of Cationic Palladium(II) Hydride Complexes *trans*-$[HPd(PPh_3)_2(DMF)]^+$ in the Oxidative Addition of Carboxylic Acids to $Pd^0(PPh_3)_4$ Observed by Conductivity Measurements in DMF

As developed by Trost et al.,[33] palladium-catalyzed reactions involving alkynes (e.g., cycloisomerization of enynes,

isomerization of alkynes to 1,3-dienes) are initiated by the reaction of a carboxylic acid HA (acetic or formic acid) with a Pd^0L_n complex (L = monophosphane ligand). A stoichiometric amount of formic acid is required in the Pd-catalyzed hydrocarboxylation of alkynes,[34] or hydrocarbonylation of aryl halides.[35]

The reaction of a carboxylic acid HA with Pd^0L_n was supposed to generate a hydridopalladium complex $[HPd^{II}AL_{n'}]$ [Equation (17)][36] that initiates the catalytic cycle by a *syn*-hydropalladation of the alkyne to form an (η^1-vinyl)palladium(II) complex as a key intermediate for further steps [Equation (18)].[33a,33b]

$$Pd^0L_n + HA \longrightarrow HPdAL_{n'} + (n\text{-}n')L \quad (17)$$

$$HPdAL_{n'} + R{-}\equiv \longrightarrow \begin{matrix} R \\ \diagdown \\ PdAL_{n'} \end{matrix} \!\!=\!\!\begin{matrix} \\ \diagup \\ H \end{matrix} \quad (18)$$

When weak carboxylic acids are considered (acetic or formic acid), the reaction is considered as an oxidative addition, i.e., insertion of Pd^0 into the H−A bond [Equation (17)].[33a,33b] Initially, it was not clear, however, whether the anion A^- remained ligated to the Pd^{II} atom or not. In 1993, Zargarian and Alper proposed the formation of cationic palladium hydride complexes $[HPd(PR_3)_2(\eta^2\text{-alkyne})]^+HCO_2^-$ in the Pd-catalyzed hydrocarboxylation of alkynes in the presence of formic acid.[34] In 1998, Trost proposed in a review the involvement of cationic complexes $[HPdL_{n''}]^+$ (rather than $[HPd(OAc)L_{n'}]$) "undoubtedly formed to some extent, albeit in an unfavorable equilibrium".[33c] Neither $HPd(OAc)L_{n'}$ nor $[HPdL_{n''}]^+$ was characterized in this context.

III.1 Evidence for the Formation of *trans*-$[HPd(PPh_3)_2(DMF)]^+A^-$ ($A^- = CH_3CO_2^-$, HCO_2^-) by Conductivity Measurements in DMF

The reaction of $Pd^0(PPh_3)_4$ with acetic acid in DMF at 25 °C was monitored by conductivity measurements.[37] The conductivity κ of a solution of $Pd^0(PPh_3)_4$ (2 mM) increased after addition of *n* equiv. of acetic acid ($n > 1$) and reached a limiting value (named κ_{equil} in Figure 4) that increased when *n* was increased up to 100. The limiting values were lower in the presence of excess PPh_3 (Figure 4).

The conductivity of acetic acid (a weak acid in DMF, $pK_a = 13.5$) was measured independently in DMF at 25 °C and was found to be negligible (e.g., 6.9 μS·cm^{-1} at 200 mM) compared to that observed when acetic acid was added to $Pd^0(PPh_3)_4$ in DMF (Figure 4).

These experiments establish that the reaction of $Pd^0(PPh_3)_4$ with acetic acid gives ionic species, which are observed to be involved in an equilibrium with the reagents because the concentration of the ionic species increased with the concentration of acetic acid. PPh_3 was involved in the backward reaction of this equilibrium. Since $Pd^0(PPh_3)_3$ is the major complex in solution,[23] the overall equilibrium observed is described in Equation (19). The inhibiting effect of PPh_3 indicates that $SPd^0(PPh_3)_2$ is the reactive species,

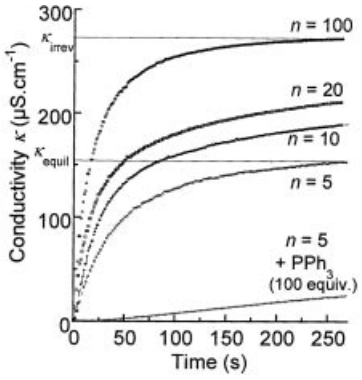

Figure 4. Conductivity in DMF of $[HPd(PPh_3)_2(DMF)]^+AcO^-$ generated in the reaction of $Pd^0(PPh_3)_4$ (2 mM) with *n* equiv. of acetic acid: $n = 100$, 20, 10, and 5 in the absence of PPh_3, or $n = 5$ in the presence of 100 equiv. of PPh_3 (as indicated in the Figure) at 25 °C

since it occurs in regular oxidative additions [Equations (20) and (21)].[22]

$$Pd^0L_3 + HA \underset{k_b}{\overset{k_f}{\rightleftharpoons}} HPdL_2S^+ + A^- + L \qquad K \quad (19)$$

$$Pd^0L_3 \rightleftharpoons SPd^0L_2 + L \quad (20)$$

$$SPd^0L_2 + HA \rightleftharpoons HPdL_2S^+ + A^- \quad (21)$$

The structure of the cationic complex *trans*-$[HPd^{II}(PPh_3)_2(DMF)]^+$ was established by NMR spectroscopy (Table 2).[37] The very negative ^1H NMR spectroscopic chemical shift suggests a hydride character for the H atom ligated to the Pd^{II} atom. The unique ^{31}P NMR spectroscopic singlet indicates that the Pd^{II} center is ligated by only two equivalent PPh_3 units that are situated in a relative *trans* position and that the fourth coordination site is occupied by the solvent. This situation differs from that of $[HPd(PPh_3)_3]^+[CH(SO_2CF_3)_2]^-$ generated in nonpolar solvents such as toluene,[38] or $[HPd(PPh_3)_3]^+CF_3CO_2^-$ generated in aqueous CF_3CO_2H, in which the palladium(II) species is ligated by three phosphane units.[39]

The reaction of $Pd^0(PPh_3)_4$ with formic acid was also monitored by conductivity measurements.[35] the experiments were performed, however, at 0 °C because of a lack of stability observed at 25 °C.[40] The reaction gave the cationic complex *trans*-$[HPd(PPh_3)_2(DMF)]^+$, with HCO_2^- as the counteranion, by a reversible process (Table 2). The overall equilibrium, expressed in Equation (19), was fully positioned to its right-hand side in the presence of 70 equiv. of formic acid.

Consequently, a cationic palladium(II) hydride *trans*-$[HPd(PPh_3)_2(DMF)]^+$ is formed in a reversible reaction, either from acetic acid or from formic acid [Equation (19)]. The molar conductivity Λ_M was calculated for the two complexes $[HPd(PPh_3)_2(DMF)]^+CH_3CO_2^-$ and $[HPd(PPh_3)_2(DMF)]^+HCO_2^-$ (Table 2).

Table 2. Characterization of the cationic hydridopalladium(II) complex $[HPd(PPh_3)_2(DMF)]^+$ formed in the oxidative addition of carboxylic acids AH to $Pd^0(PPh_3)_4$ (c_0 = 2 mM) in DMF, as well as equilibrium and rate constants [Equation (19)]

AH	Molar conductivity Λ_M [S·cm^{-2}·mol^{-1}]	^{1}H NMR [ppm][a]	^{31}P NMR [ppm][b]	K	k_f [M^{-1}·s^{-1}] (k_b) [M^{-2}·s^{-1}]
CH_3CO_2H	$[HPdL_2(DMF)]^+$, $CH_3CO_2^-$ 135 (± 5)[c]	−7.48 (br. s)	20.77 (s)	0.5×10^{-3}[c]	0.28[c] (560)[c]
HCO_2H	$[HPdL_2(DMF)]^+$, HCO_2^- 110 (± 5)[d]	−7.28 (br. s)	20.97 (s)	10^{-3}[d]	0.012[d] (12)[d]

[a] 400 MHz; shifts are referred to TMS. Solvent: $CDCl_3$ containing 10% of DMF. [b] 163 MHz; shifts are referred to H_3PO_4 as an external reference. Solvent: DMF containing 10% [D_6]acetone. [c] 25 °C. [d] 0 °C.

III.2 Determination of the Equilibrium and Rate Constants of the Oxidative Addition of Acetic or Formic Acid to $Pd^0(PPh_3)_4$ in DMF by Conductivity Measurements

III.2.1 Determination of the Equilibrium Constant K

The reaction of acetic or formic acid (n equiv.) with $Pd^0(PPh_3)_4$ obeys the general Equation (19). The equilibrium constant K was determined from the conductivity data, since the limiting values of the conductivity κ_{equil} (Figure 4) provide the thermodynamic concentration of $[HPd(PPh_3)_2(DMF)]^+$ and AcO^- at various concentrations of acetic acid.[37]

$$K = [HPdL_2(DMF)^+][A^-][L]/[Pd^0L_3][HA] = c_0 \cdot x_{equil}^2(1 + x_{equil})/(1 - x_{equil})(n - x_{equil})$$

c_0: initial concentration of $Pd^0(PPh_3)_4$; $x_{equil} = \kappa_{equil}/\kappa_{irrev}$; κ_{equil}: final conductivity measured when the equilibrium is fully established in the presence of n equiv. of HA ($t > 250$ s, Figure 4); κ_{irrev}: final conductivity measured when the equilibrium is fully positioned on its right-hand side, $n = 100$ for CH_3CO_2H (Figure 4), $n = 70$ for HCO_2H.

Identical values for K were found, whatever concentration range was investigated for each carboxylic acid ($0 < n < 100$ for acetic acid and $0 < n < 70$ for formic acid). This result establishes that the cation and anion are free ions in DMF.[37] The values of the equilibrium constants K for acetic and formic acid are gathered in Table 2. Even though they were determined at slightly different temperatures, one notices that, at identical concentrations of acids, the equilibrium lies more in favor of the cationic palladium hydride for formic acid than it does for acetic acid, which is in agreement with the fact that formic acid is slightly more acidic than acetic acid.

III.2.2 Determination of Rate Constants k_f and k_b

Acetic acid is a weak acid in DMF and the concentration of protons is negligible (vide supra) when compared to the Pd^0 concentration. This situation, however, does not exclude the possibility of a direct protonation of $Pd^0(PPh_3)_2$ to form $[HPd(PPh_3)_2S]^+$. The two pathways — (i) direct protonation of $Pd^0(PPh_3)_2$ by H^+ or (ii) oxidative addition of acetic acid to $Pd^0(PPh_3)_2$ to form $HPd(OAc)(PPh_3)_2$ followed by a fast ionization step — may be discriminated by determining the reaction order in acetic acid for the forward reaction [Equation (19)]. That is to say, a reaction order of 1/2 for CH_3CO_2H would suggest the protonation route and a reaction order of 1 for CH_3CO_2H would suggest the oxidative addition route.

The equilibrium in Equation (19) was completely shifted towards the cationic complex $[HPdL_2(DMF)]^+$ when 100 equiv. of acetic acid were treated with $Pd^0(PPh_3)_4$ (c_0 = 2 mM) in DMF. Consequently, the uppermost curve in Figure 4 is representative of the rate of formation of the cationic complex $[HPdL_2(DMF)]^+$. This kinetic curve did not exhibit any induction period, which would result in a significant accumulation of a neutral intermediate species. Moreover, the reaction was found to be faster when the concentration of acetic acid was increased (vide infra). Consequently, the intermediate neutral complex $HPd(OAc)(PPh_3)_2$, if formed in the reaction of acetic acid with $Pd^0(PPh_3)_2$, did not accumulate. Thus, the ionization of $HPd(OAc)(PPh_3)_2$ to $[HPd(PPh_3)_2(DMF)]^+$ and AcO^- was faster than its formation from $Pd^0(PPh_3)_4$, and the rate of formation of the ionic species was the same as that of the disappearance of the Pd^0 complex. Consequently, the rate constant of the forward reaction [k_f in Equation (19)] was determined using the conductivity data of the uppermost curve in Figure 4 ($n = 100$ for CH_3CO_2H). When starting from $Pd^0(PPh_3)_4$, the concentration of PPh_3 was not constant [Equation (20)] and the kinetic law is: $2\ln(1 - x_t) + x_t = -k_{obsd.} \cdot t = -k_f \cdot [HA]^\alpha t$ ($x_t = \kappa_t/\kappa_{irrev}$; κ_t = conductivity at time t; κ_{irrev} = final conductivity; α = reaction order in HA). The values of $k_{obsd.}$ were calculated for acetic acid (Figure 5, a) and formic acid from the slope of the regression line obtained by plotting $[2\ln(1 - x_t) + x_t]$ against time (Figure 5, b).[37]

The reaction of $Pd^0(PPh_3)_4$ with acetic acid was rather fast (uppermost curve in Figure 4) and, consequently, only two concentrations of acetic acid could be tested ($n = 100$: $k_{obsd.} = 0.057$ s^{-1}; $n = 200$: $k_{obs} = 0.104$ s^{-1}). From these results, it appears that the reaction order α in acetic acid is close to 1 ($k_{obsd.} = k_f \cdot [HA]$), which favors the pathway of an oxidative addition of acetic acid to $SPd^0(PPh_3)_2$ followed by a fast ionization step of the neutral complex $HPd(OAc)(PPh_3)_2$. The values of k_f were then determined for acetic and formic acid (Table 2).[37] The values of the

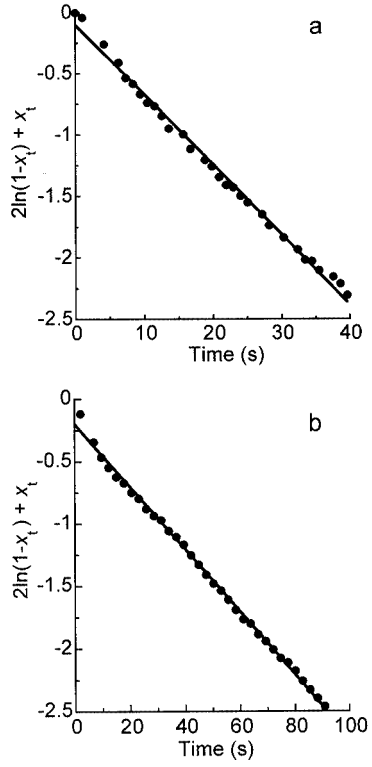

Figure 5. Kinetics of the oxidative addition of $Pd^0(PPh_3)_4$ (2 mM) in DMF to: (a) acetic acid (0.2 M) at 25 °C; (b) formic acid (0.2 M) at 0 °C; in both figures, plot of $[2\ln(1 - x_t) + x_t]$ versus time; $x_t = \kappa_t/\kappa_{irrev}$; κ_t = conductivity at t; κ_{irrev} = final conductivity, under conditions where the reactions were irreversible (see uppermost curve in Figure 4 for acetic acid)

rate constants of the backward reaction [k_b in Equation (19)] were then deduced from the values of the equilibrium constant $K = k_f/k_b$ (Table 2).

The overall equilibrium in Equation (19) may be then considered as the successive equilibria shown in Equation (22), which involve a reversible oxidative addition as the very first step (L = PPh_3).

$$Pd^0L_2 + HA \rightleftharpoons \underset{cis}{HPdAL_2} \rightleftharpoons \underset{trans}{HPdAL_2} \rightleftharpoons \underset{trans}{HPdL_2S^+} + A^- \quad (22)$$

III.3 Conclusion and Mechanistic Consequences

The results above illustrate how conductivity data may be used efficiently (i) to characterize ionic complexes formed in the reaction between a carboxylic acid and a Pd^0 complex, (ii) to establish the reversibility of this reaction and to determine its equilibrium constant, (iii) to determine the rate constant of the forward and backward reactions of the equilibrium, and (iv) to delineate the mechanism by discriminating between oxidative addition and protonation.

It has been established that a cationic palladium hydride $[HPd(PPh_3)_2(DMF)]^+$ is generated by oxidative addition of weak carboxylic acids (acetic or formic acid) and $Pd^0(PPh_3)_4$ in a coordinating solvent as DMF. However, it is generated in an unfavorable equilibrium. Consequently, as predicted by Trost,[33c] if a high concentration of the key intermediate $[HPdL_2S]^+$ is needed, a large excess of the carboxylic acid is required and use of formic acid is more efficient than acetic acid.[41]

In Heck reactions, when the precursor of the Pd^0 catalyst is $Pd(OAc)_2$ associated with phosphane ligands L, the active Pd^0 complex in the oxidative addition with PhI is the anionic species $[Pd^0L_2(OAc)]^-$, and $ArPd(OAc)L_2$ is formed in the oxidative addition of aryl iodides[16] or triflates.[15] The carbopalladation of the alkene by $ArPd(OAc)L_2$ is followed by β-hydride elimination (Scheme 11) that, according to the results just reported above, should not generate the neutral $HPd(OAc)(PPh_3)_2$ in DMF, but instead the cationic palladium hydride $[HPd(PPh_3)_2(DMF)]^+$ with AcO^- as the counteranion (Scheme 11). Since the reversibility of the oxidative addition of the acetic acid with $Pd^0(PPh_3)_2$ has been established [Equation (22)], however, the complex $[HPd(PPh_3)_2(DMF)]^+AcO^-$ must be involved in an equilibrium with acetic acid and Pd^0L_2, so that the Pd^0L_2 complex should be generated in the absence of a base. The role of the base would then be devoted to its reaction with acetic acid to generate AcO^- as a key ligand for the active complexes $[Pd^0L_2(OAc)]^-$ and $ArPd(OAc)L_2$.[16]

IV. Reversible Formation of Cationic $[(\eta^3\text{-allyl})PdL_2]^+$ Complexes in the Oxidative Addition of Allylic Carboxylates or Carbonates to Pd^0 Complexes Observed by Conductivity Measurements in DMF

Palladium complexes are efficient catalysts for Tsuji−Trost reactions, i.e., nucleophilic substitutions on allylic carboxylates[3] or carbonates[42] (R′ = OR′′) [Equation (23)].

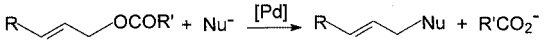

(23)

The first step of the catalytic cycle is an oxidative addition of the allylic derivative, allylOCOR′, to a lowly ligated Pd^0 complex, Pd^0L_2 (L = monodentate phosphane ligand or L_2 = bidentate phosphane ligand) [Equation (24)], which is believed to proceed in two successive steps.[3]

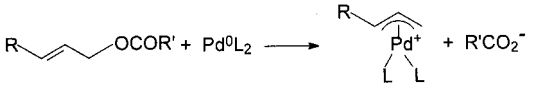

(24)

The first of these steps is a reversible complexation of the C=C double bond of the allylic derivative to Pd^0L_2 [Equation (25)]; the second step is the oxidative addition (commonly named the "ionization step") in which a cationic $[(\eta^3\text{-allyl})Pd^{II}L_2]^+$ complex is formed with the leaving group $R'CO_2^-$ as the counteranion [Equation (26)].

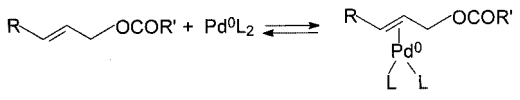

(25)

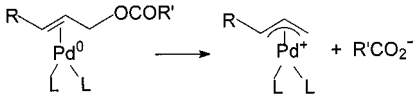

(26)

The mechanism of the next step, the nucleophilic attack onto the cationic $[(\eta^3\text{-allyl})PdL_2]^+$ complex has been widely investigated [Equation (27)].[3] Such reactions have been usually performed, however, on cationic palladium(II) complexes that were not generated in the oxidative addition of Equation (24),[43] but instead independently synthesized from dimeric $Pd_2(\eta^3\text{-allyl})_2(\mu\text{-Cl})_2$ complexes[43b] by addition of monodentate or bidentate phosphanes and abstraction of the chloride ion by MY (M = K, Na, Ag; Y = BF_4, BPh_4, OTf) [Equation (28)].[43b,44a] Under such conditions, the counteranion is BF_4^-, BPh_4^- or TfO^-, but not $R'CO_2^-$ as it would be in the oxidative addition performed from allylOCOR′. The complex [(2-methylallyl)$Pd(PPh_3)_2]^+BF_4^-$ has been characterized by conductivity measurements in aqueous acetone;[44a] the conductivity of related complexes in THF is very low.[44b] A few complexes [(1,3-diphenyl-η^3-allyl)Pd(P,P)]$^+AcO^-$ (P,P: ferrocenylphosphane ligands) have been synthesized from $Pd_2(\eta^3\text{-allyl})_2(\mu\text{-OAc})_2$, but at low temperatures.[45]

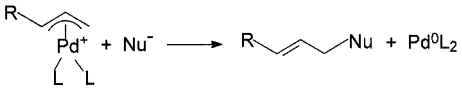

(27)

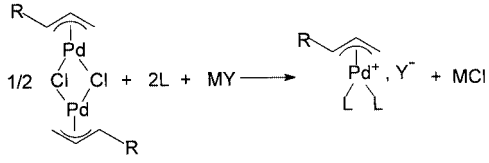

(28)

Consequently, until 1999 the cationic character of $[(\eta^3\text{-allyl})PdL_2]^+$ complexes, generated in the oxidative addition of allylic acetates with AcO^- as counteranion [Equation (24)], had never been established. Such complexes have recently been characterized by conductivity measurements in DMF with monodentate and bidentate phosphane ligands.[46−50] In addition, the reversibility of the oxidative addition has also been established by conductivity measurements in conjunction with other analytical techniques (vide infra).[46−50]

The Pd^0 precursor investigated was $Pd^0(dba)_2$ (dba: *trans*,*trans*-dibenzylideneacetone) associated with either 2 equiv. of a monophosphane ligand (L = PPh_3)[51] or with 1 equiv. of a bidentate bis(phosphane) (P,P) ligand {dppb [1,4-bis(diphenylphosphane)butane] or dppf [1,4-bis(diphenylphosphanyl)ferrocene)}[52] which are catalytic precursors for the Tsuji−Trost reactions.[3,51]

IV.1 Reversible Formation of Cationic $[(\eta^3\text{-allyl})PdL_2]^+$ Complexes in the Oxidative Addition of Allyl Acetate to Pd^0 Complexes Ligated by a Monophosphane Ligand

The reaction of $Pd^0(dba)_2$ with 2 equiv. of PPh_3 in DMF or THF gives the major complex $Pd^0(dba)(PPh_3)_2$. The species is involved in an equilibrium with the minor complex $SPd^0(PPh_3)_2$, the usual active species in oxidative additions (Scheme 13).[53]

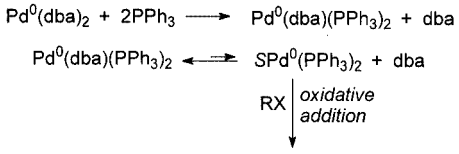

Scheme 13. Mechanism of the oxidative addition of an electrophile RX with the Pd^0 complex generated from the catalytic precursors $Pd^0(dba)_2$ and PPh_3 (2 equiv.) in DMF or THF

Conductivity measurements were performed on a solution of $Pd^0(dba)_2$ (c_0 = 2 mM) and 2 equiv. of PPh_3 in DMF after addition of 6.2 equiv. of $CH_2{=}CHCH_2OAc$. The conductivity κ increased with time to reach a plateau (κ_{equil}) whose value increased upon successive additions of allyl acetate (Figure 6, a).[46] This observation establishes that ionic species were formed that were involved in an equilibrium with the starting reagents [Equation (29)] because their concentration increased upon increasing the allyl acetate concentration. The conductivity κ_{equil} decreased when the concentration of dba was increased (Figure 6, b). Consequently, dba is involved in the reverse reaction of the equilibrium [Equation (29)].[46]

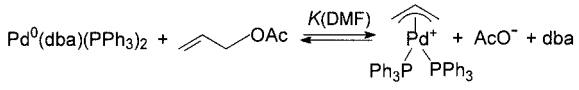

(29)

The complex $[(\eta^3\text{-}CH_2CHCH_2)Pd(PPh_3)_2]^+$ formed in the reaction was identified by a singlet in the ^{31}P NMR spectrum at δ = 24.06 ppm; by comparison, an authentic sample of $[(\eta^3\text{-}CH_2CHCH_2)Pd(PPh_3)_2]^+BF_4^-$ has δ = 24.08 ppm.[44a] The reversibility of the equilibrium in Equation (29) was established independently by treating $[(\eta^3\text{-}CH_2CHCH_2)Pd(PPh_3)_2]^+BF_4^-$ with 1 equiv. of nBu_4NOAc in the presence of 2 equiv. of dba. The complex $Pd^0(dba)(PPh_3)_2$ formed in the backward reaction was characterized by ^{31}P NMR spectroscopy when the reaction was performed in DMF, whereas $CH_2{=}CHCH_2OAc$ was characterized by ^1H NMR spectroscopy when the reaction was performed in $CDCl_3$.[46]

The equilibrium constant K_{DMF} [Equation (29)] could have been determined using the conductivity data of Figure 6 (a), as was accomplished for $[HPd(PPh_3)_2(DMF)]^+AcO^-$ (see Sect. III.2.1). The full shift, however, of the equilibrium towards the ionic species required a larger amount of allyl acetate ($n >> 100$) than that used in Figure 6 (a). Consequently, the intrinsic con-

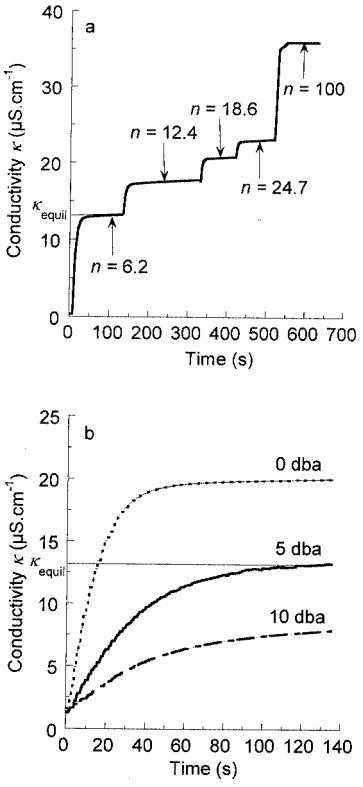

Figure 6. (a) Conductivity in DMF of $[(\eta^3\text{-}CH_2CHCH_2)Pd(PPh_3)_2]^+AcO^-$ formed in the reaction of the Pd^0 complex generated from $Pd^0(dba)_2$ (2 mM) and PPh_3 (4 mM) with $CH_2{=}CHCH_2OAc$ added successively at 20 °C; as indicated, n is the cumulative number of equiv. of $CH_2{=}CHCH_2OAc$; (b) conductivity of $[(\eta^3\text{-}CH_2CHCH_2)Pd(PPh_3)_2]^+AcO^-$ generated in the reaction of $Pd^0(dba)_2$ (2 mM) and PPh_3 (4 mM) with $CH_2{=}CHCH_2OAc$ (0.1 M) at 20 °C, in the presence of various amounts of dba, which was added to $Pd^0(dba)_2$ and PPh_3 prior the introduction of $CH_2{=}CHCH_2OAc$

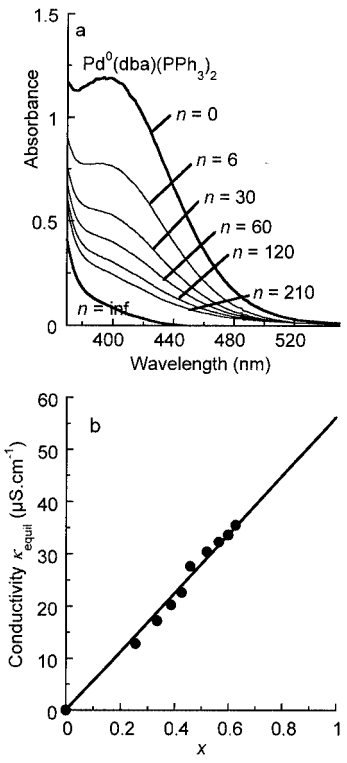

Figure 7. (a) UV spectrum performed in a 1-mm path cell of a solution of $Pd^0(dba)_2$ (1 mM) and PPh_3 (2 mM) in the presence of n equiv. of $CH_2{=}CHCH_2OAc$ in DMF at 20 °C; (b) plot of the conductivity κ_{equil}, measured for various values of n in Figure 6 (a), versus the corresponding molar fraction x calculated from the value of the equilibrium constant K [Equation (29)]; the molar conductivity Λ_M of $[(\eta^3\text{-}CH_2CHCH_2)Pd(PPh_3)_2]^+AcO^-$ was determined by extrapolation to $x = 1$

ductivity κ of $[(\eta^3\text{-}CH_2CHCH_2)Pd(PPh_3)_2]^+$ and AcO^- could not be determined from Figure 6 (a). The equilibrium constant $K_{DMF} = [(\eta^3\text{-}C_3H_5)PdL_2^+][AcO^-][dba]/[Pd^0(dba)L_2][CH_2{=}CHCH_2OAc]$ was determined easily by UV spectroscopy, taking advantage of the absorbance of $Pd^0(dba)(PPh_3)_2$ (λ_{max} = 396 nm) in DMF (Figure 7, a).

Successive additions of the allyl acetate resulted in successive additional decays of the absorbance of $Pd^0(dba)(PPh_3)_2$ (Figure 7, a), which provides further evidence for the equilibrium in Equation (29). At a given wavelength, the thermodynamic concentration of $Pd^0(dba)(PPh_3)_2$ was given by the ratio $(D_{equil} - D_{inf})/(D_0 - D_{inf})$ at different allyl acetate concentrations with $(D_{equil} - D_{inf})$ being the absorbance of $Pd^0(dba)(PPh_3)_2$ at the equilibrium position and $(D_0 - D_{inf})$ being the initial absorbance of $Pd^0(dba)(PPh_3)_2$.[46]

$K_{DMF} = 3.5\ (\pm\ 0.4) \times 10^{-5}$ M (20 °C)

One notices in Figure 7 (a) that more than 100 equiv. of allyl acetate were required to completely shift the equilibrium towards the cationic complex. From the value of K_{DMF}, the molar fraction x of the cationic complex could be calculated for each value of n used in the conductivity measurements of Figure 6 (a). The plot of κ_{equil} (determined in Figure 6, a) versus x was linear (Figure 7, b), which confirms the formation of the free ions $[(\eta^3\text{-}CH_2CHCH_2)Pd(PPh_3)_2]^+$ and AcO^- in DMF. The molar conductance was determined by extrapolation to $x = 1$.

$\Lambda_M = 56\ (\pm\ 2)$ S·cm^{-2}·mol^{-1} for
$[(\eta^3\text{-}CH_2CHCH_2)Pd(PPh_3)_2]^+AcO^-$ in DMF at 20 °C

No conductivity was observed in THF, but clearly the reaction took place since the UV absorbance of $Pd^0(dba)(PPh_3)_2$ (λ_{max} = 394 nm) decreased stepwise upon successive additions of the allyl acetate, as had been observed in DMF. Moreover, the resulting cationic complex $[(\eta^3\text{-}CH_2CHCH_2)Pd(PPh_3)_2]^+$ was characterized by ^{31}P NMR spectroscopy (δ = 24.5 ppm) in THF. Consequently, non-dissociative ion pairs $[(\eta^3\text{-}CH_2CHCH_2)\text{-}Pd(PPh_3)_2{}^+AcO^-]$ are formed in THF [Equation (30)], whereas free ions were formed in DMF [Equation (29)]. The equilibrium constant K_{THF} was determined by UV spectroscopy.

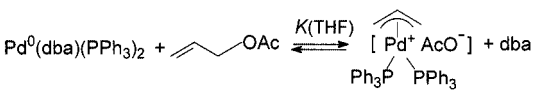

(30)

$K(THF) = 1\ (\pm\ 0.4) \times 10^{-3}$ (20 °C)

One notices that for the same concentration of Pd^0 (c_0 = 1 mM), the equilibrium lies more in favor of the cationic complex in DMF than it does in THF.[46]

In both solvents, DMF and THF, we observe an overall equilibrated reaction from $Pd^0(dba)(PPh_3)_2$, but it is a multistep process (Scheme 14, R′ = Me). Indeed, the three initially sharp signals in the ^1H NMR spectrum of the allyl ligand of $[(\eta^3\text{-}CH_2CHCH_2)Pd(PPh_3)_2]^+BF_4^-$ observed in $CDCl_3$ became broad after addition of 1 equiv. of nBu$_4$NOAc and 2 equiv. of dba, and sharp signals of CH_2=$CHCH_2OAc$ (formed by attack of acetate ions on the allyl ligands) appeared. The presence of both broad and sharp signals in the same ^1H NMR spectrum indicates that different equilibria are operating with different equilibration rates. Consequently, the oxidative addition involves at least two steps and probably proceeds via the intermediate postulated in the literature, complex $Pd^0(\eta^2\text{-}CH_2$=$CHCH_2OAc)(PPh_3)_2$, which could not be detected when PPh_3 is the ligand for the palladium center. Clear-cut evidence for the intermediates is provided in the reactions with allylic benzoates or with bidentate ligands (see Sect. IV.3 and IV.2, respectively).

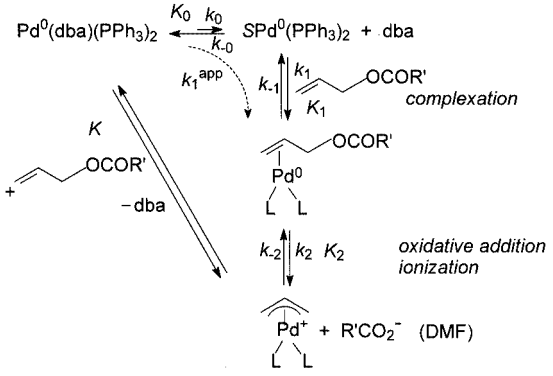

Scheme 14. Mechanism of the reversible reaction of allyl carboxylates with the Pd^0 complexes generated from $Pd^0(dba)_2$ and PPh_3 (2 equiv.) in DMF

Consequently, the overall equilibrium between $Pd^0(dba)(PPh_3)_2$, CH_2=$CHCH_2OAc$ and the cationic complex $[(\eta^3\text{-}CH_2CHCH_2)Pd(PPh_3)_2]^+AcO^-$ involves three successive equilibria (Scheme 14, R′ = Me) with K = $K_0{\cdot}K_1{\cdot}K_2$.

Compared to the postulated mechanisms in Equations (25) and (26), we now have clear evidence that the reaction of an allyl acetate with a Pd^0 complex is a reversible reaction, which leads to a cationic $[(\eta^3\text{-allyl})Pd(PPh_3)_2]^+$ complex with AcO^- as the counteranion. This result demonstrates unambiguously that the true oxidative addition (ionization step) is a reversible reaction (with K_2 as its equilibrium constant, Scheme 14, R′ = Me). Consequently, the acetate ion is not an "innocent" leaving group since it reacts with the cationic $[(\eta^3\text{-allyl})Pd(PPh_3)_2]^+$ complex to give back the allylic acetate and a Pd^0 complex.[46]

This conclusion is in agreement with a few reports in the literature that have suggested that the oxidative addition step is reversible. Indeed, in the absence of any nucleophile, isomerization of the C=C bond of allylic acetates had been observed as well as isomerization at the allylic position in substituted cyclic allylic acetates.[54]

IV.2 Reversible Formation of Cationic $[(\eta^3\text{-allyl})PdL_2]^+$ Complexes in the Oxidative Addition of the Allyl Acetate to Pd^0 Complexes Ligated by Bidentate Bis(phosphanes)

The reaction of $Pd^0(dba)_2$ with 1 equiv. of a bidentate P,P ligand in DMF or THF gives the major complex $Pd^0(dba)(P,P)$. This complex is involved in an equilibrium with the minor complex SPd^0(P,P), which is the more reactive species in oxidative additions (Scheme 15).[53b,55]

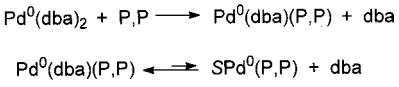

Scheme 15. Pd^0 complexes generated from $Pd^0(dba)_2$ and 1 equiv. of a bidentate P,P ligand in DMF or THF

The reaction of CH_2=$CHCH_2OAc$ with the Pd^0 complexes generated from $Pd^0(dba)_2$ (c_0 = 2 mM) and dppb (2 mM) in DMF was monitored by conductivity measurements to characterize the formation of ionic species.[47] The conductivity increased with time after addition of 5 equiv. of allyl acetate and reached a limiting value (Figure 8, a). This limiting value increased slightly after addition of a further 5 equiv. of allyl acetate, but remained unchanged after addition of yet another 5 equiv. of allyl acetate. The limiting conductivity (κ_{equil}) decreased upon successive additions of dba (Figure 8, a). These experiments establish that ionic species form that are involved in an equilibrium with the starting reagents, whereas dba is involved in the backward reaction [Equation (31)].

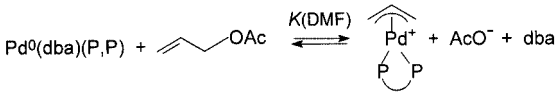

(31)

The complex formed in the oxidative addition was characterized by ^{31}P NMR spectroscopy [δ = 21.5 ppm (s)] and its structure was assigned to the cationic complex $[(\eta^3\text{-}CH_2CHCH_2)Pd(dppb)]^+AcO^-$ by comparison with an authentic sample of $[(\eta^3\text{-}CH_2CHCH_2)Pd(dppb)]^+BF_4^-$ [δ = 21.7 ppm (s)]. The molar conductance Λ_M of $[(\eta^3\text{-}CH_2CHCH_2)Pd(dppb)]^+AcO^-$ was determined from the value of κ_{irrev} (Figure 8, a) obtained when the equilibrium was fully shifted to the side of formation of the ionic species (15 equiv. allyl acetate). At this point, its concentration was c_0 = 2 mM, i.e., the initial Pd^0 concentration.

Λ_M = 42 (± 2) S·cm^{-2}·mol^{-1} for $[(\eta^3\text{-}CH_2CHCH_2)Pd(dppb)]^+AcO^-$ in DMF at 25 °C

The backward reaction of the equilibrium in Equation (31) was monitored by UV and ^{31}P NMR spectroscopy.

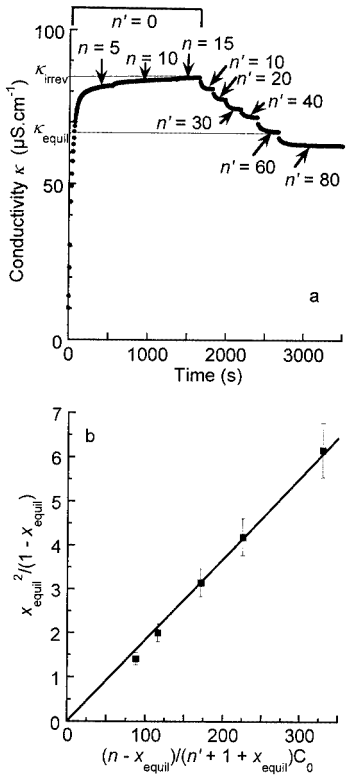

Figure 8. (a) Conductivity in DMF of $[(\eta^3\text{-}CH_2CHCH_2)Pd(dppb)]^+AcO^-$ formed in the reaction of the Pd^0 complex, generated from $Pd^0(dba)_2$ (2 mM) and dppb (2 mM), with $CH_2{=}CHCH_2OAc$ added successively ($0 < t < 1500$ s) at 25 °C; as indicated by the arrows, n is the cumulative number of equiv. of $CH_2{=}CHCH_2OAc$; this addition is followed by successive additions of dba ($t > 1500$ s); as indicated by the arrows, n' is the cumulative equiv. of added dba; (b) determination of the equilibrium constant K [Equation (31)] using the conductivity data of Figure 8 (a); plot of $[x^2_{equil}/(1 - x_{equil})]$ versus $[(n - x_{equil})/(n' + 1 + x_{equil})c_0]$. The value of $x_{equil} = \kappa_{equil}/\kappa_{irrev}$ [κ_{equil}: conductivity measured when the equilibrium in Equation (31) is fully established in the presence of n equiv. of $CH_2{=}CHCH_2OAc$ and n' equiv. of dba ($n = 5$ with $n' = 0$; $n = 15$ with $10 \le n' \le 80$; κ_{irrev}: conductivity when the equilibrium in Equation (31) is totally displaced towards its right-hand side in the absence of added dba ($n = 15$, $n' = 0$)]; K is determined from the slope

The UV spectrum of a solution of $[(\eta^3\text{-}CH_2CHCH_2)Pd(dppb)]^+BF_4^-$ (2 mM) in DMF exhibited, after addition of 5 equiv. of dba and 5 equiv. of nBu$_4$NOAc, an absorption band at $\lambda_{max} = 385$ nm that is characteristic of $Pd^0(dba)(dppb)$. Two broad signals in the ^{31}P NMR spectrum of $Pd^0(dba)(dppb)$ were also observed ($\delta = 21.17$ and 18.0 ppm).[55] These experiments provide clear evidence that the acetate ions react with the cationic complex $[(\eta^3\text{-}CH_2CHCH_2)Pd(dppb)]^+$ to generate a Pd^0 complex.[47]

IV.2.1 Determination of the Equilibrium Constant in DMF by Conductivity Measurements

The equilibrium constant K_{DMF} of the overall equilibrium [Equation (31)] was determined using the conductivity measurements of Figure 8 (a). The molar fraction x of the cationic complex in the equilibrium is given by $x_{equil} = \kappa_{equil}/\kappa_{irrev}$ for various values of n (equiv. of allyl acetate) and n' (equiv. of added dba).

$$K_{DMF} = [(\eta^3\text{-}CH_2CHCH_2)Pd(dppb)^+][AcO^-]\text{-}[dba]/[Pd^0(dba)(dppb)][CH_2{=}CHCH_2OAc]$$

$$K_{DMF} = c_0{\cdot}x^2_{equil}(n' + 1 + x_{equil})/(1 - x_{equil})(n - x_{equil})$$

Plotting $[x^2_{equil}/(1 - x_{equil})]$ versus $[(n - x_{equil})/(n' + 1 + x_{equil})c_0]$ gave a straight line with K_{DMF} as the slope (Figure 8, b): $K_{DMF} = 1.8 \times 10^{-2}$ M at 25 °C (Table 3, Entry 19). The equilibrium constant K was similarly calculated for the reaction involving the ligand dppf (Table 3, Entries 16, 17).[47]

Table 3. Effect of the leaving group $-OCOR'$ on the kinetics and thermodynamics of the reaction of allyl carboxylates[a] with the Pd^0 complexes generated from $Pd^0(dba)_2$ ($c_0 = 1$ mM) and 2 equiv. of PPh_3 (Scheme 14) or $Pd^0(dba)_2$ ($c_0 = 2$ mM) and 1 equiv. of dppf or dppb (Scheme 16) in DMF; comparative equilibrium constants K and rate constants k_1^{app}, K_0k_1, and k_2

Entry	$CH_2{=}CHCH_2{-}OCOR'$	Ligand	T [°C]	$10^3 \times K$ [M]	k_1^{app} [$M^{-1}s^{-1}$]	K_0k_1 [s^{-1}]	k_2 [s^{-1}]
1	$-OCO_2Et$	PPh_3	20	irrev.	> 100[b]	> 0.1	n.d.[c]
2	$-OCO_2Et$	PPh_3	–15	irrev.	1.5	0.0015	> 0.015
3	$-OCOCF_3$	PPh_3	–10	irrev.	40[d]	0.004	>> 1
4	$-OCOCF_3$	PPh_3	20	irrev.	> 100[b]	> 0.1	n.d.[c]
5	$-OCOCH_2Cl$	PPh_3	20	280	> 100[b]	> 0.1	n.d.[c]
6		PPh_3	20	150	> 100[b]	> 0.1	n.d.[c]
7		PPh_3	10	n.d.	80	0.08	0.5
8		PPh_3	20	8.6	62	0.062	n.d.
9		PPh_3	10	n.d.	30	0.03	0.17
10	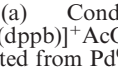	PPh_3	20	2	n.d.	n.d.	n.d.
11		PPh_3	10	n.d.	25	0.025	0.15
12	$-OCOCH_3$	PPh_3	20	0.035	n.d.	n.d.	n.d.
13	$-OCOCF_3$	dppf	16	340	> 100[b]	> 0.2	n.d.
14	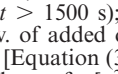	dppf	16	180	> 100[b]	> 0.2	0.021
15	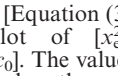	dppf	16	14	94	0.19	0.01
16	$-OCOCH_3$	dppf	16	1.1	4.8	0.019	0.018
17	$-OCOCH_3$	dppf	25	0.7	8.4	0.017	n.d.
18	$-OCOCF_3$	dppb	25	52	n.d.[c]	n.d.[c]	n.d.[c]
19	$-OCOCH_3$	dppb	25	18	26	0.1	0.025

[a] For a given ligand, the leaving groups are classified, when going down the table, in the order of their decreasing ability to leave. [b] Fast reaction: 100 $M^{-1}{\cdot}s^{-1}$ is the maximum value of the rate constant that could be determined by UV spectroscopy under our experimental conditions ($t_{1/2} = 2$ s for $c_0 = 1$ mM and [allylOCOR′] = 5 mM). [c] Not determined because the reaction is too fast. [d] For concentrations of $CH_2{=}CHCH_2OCOCF_3$ smaller than 0.02 M.[50]

Therefore, as for PPh_3, the reaction of the allyl acetate with the Pd^0 complex formed from $Pd^0(dba)_2$ and 1 equiv. of either dppb or dppf is a reversible reaction that generates cationic complexes $[(\eta^3\text{-}CH_2CHCH_2)Pd(P,P)]^+$ with AcO^- as the counteranion. The overall equilibrium, however, lies considerably more in favor of the cationic (η^3-allyl)palladium complex for the bidentate ligands dppb and dppf than it does for PPh_3 (compare the values of K in Table 3, Entries 12, 17, 19).[46,47]

IV.2.2 Determining the Rate Constants of the Complexation and Ionization Steps: Kinetic Evidence for Intermediate Neutral Complexes [$Pd^0(\eta^2\text{-}CH_2{=}CHCH_2OAc)(P,P)$]

As seen in Figure 8 (a), the overall equilibrium in Equation (31) could easily be fully displaced towards the side of the cationic complex. With 5 equiv. of $CH_2{=}CHCH_2OAc$,

the overall reaction could be considered as being almost irreversible. Under such conditions, the kinetics of the formation of the cationic complex $[(\eta^3\text{-}CH_2CHCH_2)Pd(dppb)]^+$ with AcO^- as the counteranion could be monitored by conductivity measurements in DMF (curve C in Figure 9, a). The disappearance of $Pd^0(dba)(dppb)$ was monitored by UV spectroscopy at $\lambda_{max} = 385$ nm in DMF (curve A in Figure 9, a). The rate of disappearance of $Pd^0(dba)(dppb)$ was faster ($t_{1/2} = 8$ s) than the rate of formation of the cationic complex $[(\eta^3\text{-}CH_2CHCH_2)Pd(dppb)]^+$ ($t_{1/2} = 25$ s) whose kinetic curve C was S-shaped initially (Figure 9, a). Consequently, an intermediate neutral complex was generated before the formation of the cationic complex $[(\eta^3\text{-}CH_2CHCH_2)Pd(dppb)]^+$, presumably $Pd^0(\eta^2\text{-}CH_2{=}CHCH_2OAc)(dppb)$ where the Pd^0 atom is ligated to the C=C bond of the allyl acetate, as has been postulated in the literature.[3] The evolution of this neutral complex over time was deduced from the kinetic curves A and C (curve B in Figure 9, a). The neutral complex could not be characterized spectroscopically because it has too short a lifetime, but this was the first kinetic evidence for its formation.

Consequently, the reaction of allyl acetate with the Pd^0 complex, formed from $Pd^0(dba)_2$ and 1 equiv. of dppb, is a reversible one [Equation (31)] that proceeds through three reversible steps (Scheme 16, R′ = Me) with $K = K_0{\cdot}K_1{\cdot}K_2$.[47]

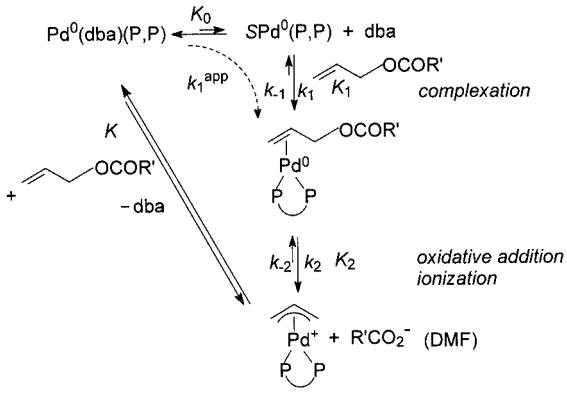

Scheme 16. Mechanism of the reversible reaction in DMF of allyl carboxylates with the Pd^0 complex formed from $Pd^0(dba)_2$ and 1 equiv. of (P,P) ligand (dppb, dppf)

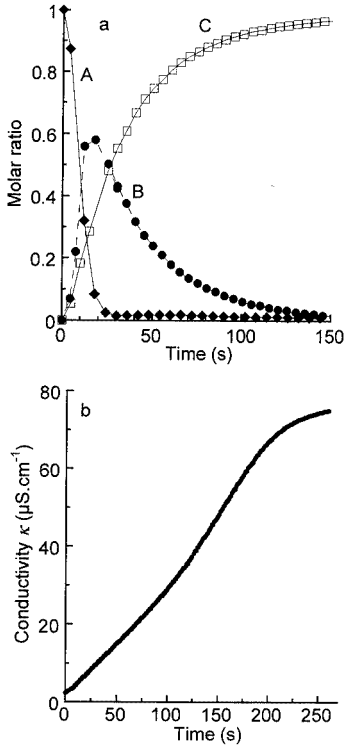

Figure 9. (a) Kinetics of the reaction of $CH_2{=}CHCH_2OAc$ (10 mM) with the Pd^0 complex formed from $Pd^0(dba)_2$ (2 mM) and dppb (2 mM) in DMF at 25 °C: A (filled diamonds): molar ratio of $Pd^0(dba)(dppb)$ versus time, determined by UV spectroscopy at 425 nm; B (filled circles): molar ratio of the neutral intermediate complex $(\eta^2\text{-}CH_2{=}CHCH_2OAc)Pd^0(dppb)$ versus time, determined from curves A and C [B = 1 − (A + C)]; C (empty squares): molar ratio of the cationic complex $[(\eta^3\text{-}CH_2CHCH_2)Pd(dppb)]^+AcO^-$ versus time, determined by conductivity measurements; (b) kinetics of the reaction of $CH_2{=}CHCH_2OAc$ (10 mM) with the Pd^0 complex formed from $Pd^0(dba)_2$ (2 mM) and dppf (2 mM) in DMF at 16 °C, monitored by conductivity measurements of the cationic complex $[(\eta^3\text{-}CH_2CHCH_2)Pd(dppf)]^+AcO^-$

Curve A in Figure 9 (a) represents the kinetics of the overall complexation step in which $Pd^0(dppb)(\eta^2\text{-}CH_2{=}CHCH_2OAc)$ is formed from $Pd^0(dba)(dppb)$ via $SPd^0(dppb)$. The values of $K_0{\cdot}k_1$ (Scheme 16) and the apparent rate constant of the overall complexation step, $k_1^{app} = K_0{\cdot}k_1/c_0$, were determined (Table 3, Entry 19).[47] A reaction order of +1 in allyl acetate was found for this step.[47]

Curve C in Figure 9 (a) represents the kinetics of the formation of the cationic complex $[(\eta^3\text{-}CH_2CHCH_2)Pd(dppb)]^+AcO^-$. Since this step is slower than the overall complexation step, the rate constant of the oxidative addition/ionization step (k_2 in Scheme 16) can be readily obtained from curve C, which is established by conductivity measurements, when $t > 30$ s (Table 3, Entry 19).[47] The rate of formation of the cationic $[(\eta^3\text{-}CH_2CHCH_2)Pd(dppb)]^+$ complex did not depend on the concentration of allyl acetate when it was in the range 0.02−0.1 M ($10 < n < 50$). This observation confirms a posteriori that the complexation and oxidative addition/ionization steps proceed successively on different timescales, with the oxidative addition/ionization step being slower (rds) than the overall complexation step. The term $k_1^{app}[CH_2{=}CHCH_2OAc] > k_2$ as soon as $[CH_2{=}CHCH_2OAc] > 1$ mM in DMF at 25 °C.[47]

Similar results were obtained when the Pd^0 precursor was formed from $Pd^0(dba)_2$ and 1 equiv. of dppf. The S-shaped curve, representative of the kinetics of formation of $[(\eta^3\text{-}CH_2CHCH_2)Pd(dppf)]^+AcO^-$, was, however, amplified (Figure 9, b) because of a smaller difference in the timescales of the complexation and ionization steps at the concentration of allyl acetate investigated here (0.1 mM). Determination of k_1^{app}, $K_0{\cdot}k_1$ and k_2 (Table 3, Entries 16, 17)

showed that $k_1^{app}[CH_2{=}CHCH_2OAc] > k_2$ as soon as $[CH_2{=}CHCH_2OAc] = 4$ mM in DMF at 16 °C.[47]

Therefore, by means of two different analytical techniques — UV spectroscopy for the complexation step and conductivity measurements for the ionization step — kinetic evidence for the formation of the intermediate complex $Pd^0(\eta^2\text{-}CH_2{=}CHCH_2OAc)(P,P)$ (P,P = dppb, dppf) has been obtained for the first time.

IV.3 Influence of the Leaving Group on the Kinetics and Thermodynamics of the Reaction of Allyl Carboxylates with Pd^0 Complexes in DMF

The influence of the leaving group $R'CO_2^-$ on the equilibrium and rate constants of the reaction of allyl carboxylates or carbonates with Pd^0 complexes has been investigated. The equilibrium constant $K = K_0{\cdot}K_1{\cdot}K_2$ of the overall equilibrium between $Pd^0(dba)L_2$ (L = PPh_3 or L_2 = dppb or dppf), allyl carboxylates or carbonates, and the ionic species, was determined by UV spectroscopy, as reported above for the case of allyl acetate, $CH_2{=}CHCH_2OAc$ (Schemes 14 and 16; Table 3).[50] The overall reaction may be irreversible in the case of very reactive allyl carboxylates, or by using a large excess of them. Under conditions of irreversibility, the apparent rate constant $k_1^{app} = K_0{\cdot}k_1/c_0$ of the overall complexation step (Schemes 14 and 16) was determined by UV spectroscopy, which provided kinetic data on the disappearance of the Pd^0 complex. The rate of formation of the cationic complex $[(\eta^3\text{-allyl})PdL_2]^+$ was monitored by conductivity measurements. The rate constant, k_2 (Schemes 14 and 16), was determined when the ionization step was rate-determining. The data are gathered in Table 3.[50]

The reaction of allyl carboxylates $CH_2{=}CHCH_2OCOR'$ was irreversible when considering very good OCOR′ leaving groups, such as carbonate and trifluoroacetate (Table 3, Entries 1−4), whatever the conditions (large excess of dba or at low temperatures). The rate constants of the chemical steps, k_1^{app} and k_2 (Scheme 14), were too fast to be determined with high precision at 20 °C. Thus, the kinetics were monitored below 0 °C (Table 3, Entries 2, 3). For $OCOCF_3$, at −10 °C, the kinetic curve of the formation of the cationic complex was exponential (not S-shaped) with a rate of formation equal to that of the rate of disappearance of $Pd^0(dba)(PPh_3)_2$. This observation means that ionization of the intermediate complex $Pd^0(\eta^2\text{-}CH_2{=}CHCH_2OCOCF_3)(PPh_3)_2$ was faster than its formation, which was, thus, rate-determining: $k_1^{app}[CH_2{=}CHCH_2OCOCF_3] < k_2$.[50] Under such conditions, monitoring the rate of formation of the cationic complex by conductivity measurements did not provide the value of k_2, but, instead, that of k_1^{app}. A reaction order of +1 was found at low concentrations of $CH_2{=}CHCH_2OCOCF_3$ whereas the reaction order was zero at higher concentrations (> 0.2 M). This observation means that at high concentrations of $CH_2{=}CHCH_2OCOCF_3$, the reaction rate was no longer determined by the complexation of $CH_2{=}CHCH_2OCOCF_3$, but by the step that delivered the reactive species $SPd^0(PPh_3)_2$ from $Pd^0(dba)(PPh_3)_2$; i.e., the forward reaction with k_0 of the first equilibrium (Scheme 14). This result allowed the determination of $k_0 = 0.17\ M^{-1}{\cdot}s^{-1}$ (DMF, −10 °C).[50] Therefore, a fast oxidative addition may be limited by a decomplexation step (here dba) that delivers the reactive lowly ligated Pd^0 complex.[18]

For less effective leaving groups, such as chloromethyl acetate, benzoates, and acetate (Table 1, Entries 5−12, 14−17, 19), the overall reaction was equilibrated and, as expected, the better the leaving group, the higher the value of *K*. Indeed, a good leaving group will favor the two forward reactions, i.e., the complexation step, because the C=C bond becomes less electron-rich, and the oxidative addition step, in which the leaving group is released. A good leaving group will also disfavor the backward reaction of the last step (rate constant k_{-2}) because of its poor ability as a nucleophile. Thus, it is a consistent observation that, for a given ligand, the rate constants k_1^{app} (or $K_0{\cdot}k_1$) and k_2 increase with increasing leaving-group ability (Table 3, Entries 7,9,11 and 15, 14).[50]

In the benzoate series ($CH_2{=}CHCH_2OBz$), the rate constants k_1^{app} and k_2 were determined at 10 °C (Table 3, Entries 7, 9, 11).[50] The kinetic curves for the formation of the cationic complexes were S-shaped for appropriate concentrations of allyl benzoates (ca. 10 mM). This observation is again evidence for the formation of the intermediate complexes $Pd^0(\eta^2\text{-}CH_2{=}CHCH_2OBz)(PPh_3)_2$ with the overall complexation step being slightly faster than the ionization step: $k_1^{app}[CH_2{=}CHCH_2OBz] > k_2$.

Therefore, the ionization step is faster than the complexation step for good leaving groups (carbonate, trifluoroacetate) and the ionization step is rate-determining for poor leaving groups (acetate, benzoates).

IV.4 Reversible Formation of Cationic $[(\eta^3\text{-allyl})PdL_2]^+$ in the Oxidative Addition of Allylic Carbonates to Pd^0 Complexes Observed by Conductivity Measurements

The palladium-catalyzed reaction of allylic carbonates may be performed with neutral pronucleophiles NuH [Equation (32)].[42]

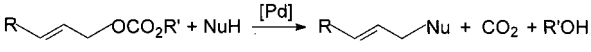

(32)

Indeed, the anion $EtOCO_2^-$, formed in the oxidative addition of the allylic carbonate to Pd^0 complexes, may decarboxylate to generate the basic EtO^- ion that is able to deprotonate NuH. As was found for allylic acetates, the oxidative addition of the allylic carbonate to Pd^0 complexes was supposed in the literature to give ionic species, i.e., a cationic $(\eta^3$-allyl)palladium(II) complex with the unstable $EtOCO_2^-$ counteranion.[56]

IV.4.1 Evidence from Conductivity Measurements in DMF for the Reversible Formation of a Cationic [(η³-allyl)PdL₂]⁺ Complex in the Oxidative Addition of a Cyclic Allylic Carbonate to Pd⁰ Complexes

Conductivity measurements were performed in DMF at 20 °C on a solution of $Pd^0(dba)_2$ (2 mM) and 2 equiv. of PPh_3 by successive addition of various amounts of the allylic carbonate *cis*-**2** (formula in Scheme 17).[57] The conductivity κ increased with time to reach a limiting value that increased when the concentration of the allylic carbonate was increased (Figure 10, a). From these experiments, it was established that ionic species are formed in an equilibrium with the allylic carbonate and $Pd^0(dba)(PPh_3)_2$. On the other hand, the conductivity decreased when dba was added (Figure 10, a), which establishes that dba is involved in the backward reaction of the equilibrium. The allylic protons of the Pd^{II} complex were characterized by ^1H NMR spectroscopy in $CDCl_3$, as were those of the $EtOCO_2^-$ anion. This anion remained unchanged after 1 h, which proves its relative stability in chloroform[56] with regards to its decarboxylation. Consequently, it is assumed that the allylic carbonate *cis*-**2** reacts with the Pd^0 complex through an overall reversible reaction with formation of a cationic complex **3** with $EtOCO_2^-$ as the counteranion [Equation (33)].[57] This complex should be a priori *trans*-**3** (left part of Scheme 17) since the overall reaction always proceed with inversion of the configuration.[3]

$$Pd^0(dba)L_2 + \underset{\mathbf{2}}{allyl\text{–}OCO_2Et} \overset{K}{\rightleftharpoons} \underset{\mathbf{3}}{(\eta^3\text{–}allyl)PdL_2^+} + EtOCO_2^- + dba \qquad L = PPh_3 \qquad (33)$$

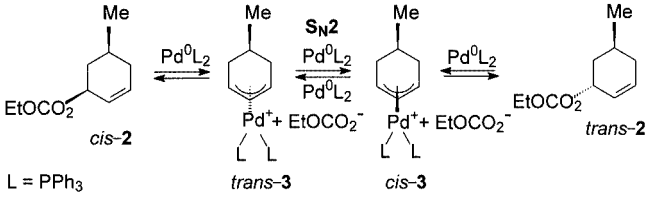

Scheme 17. Mechanism of the oxidative addition of a cyclic allylic carbonate to Pd^0L_2, whose precursor is either Pd^0L_4 or $Pd^0(dba)_2$ plus 2 equiv. of L in DMF (the solvent on Pd^0L_2 has been omitted voluntarily)

As was done with the allyl acetate (see Sect. IV.1), the equilibrium constant *K* was determined by UV spectroscopy. Indeed, addition of *n* equiv. of *cis*-**2** to $Pd^0(dba)(PPh_3)_2$ (c_0 = 1 mM), formed from $Pd(dba)_2$ and 2 equiv. of PPh_3, in DMF resulted in a fast decay of the absorbance of $Pd^0(dba)(PPh_3)_2$, which reached a constant value (Figure 10, b). Successive additions of *cis*-**2** resulted in related additional decays of the absorbance of $Pd^0(dba)(PPh_3)_2$, thus confirming that $Pd^0(dba)(PPh_3)_2$ and *cis*-**2** were involved in an equilibrium with the cationic complex **3**, dba, and $EtOCO_2^-$ [Equation (33)]. The UV spectroscopic data in Figure 10 (b) provided the thermodynamic

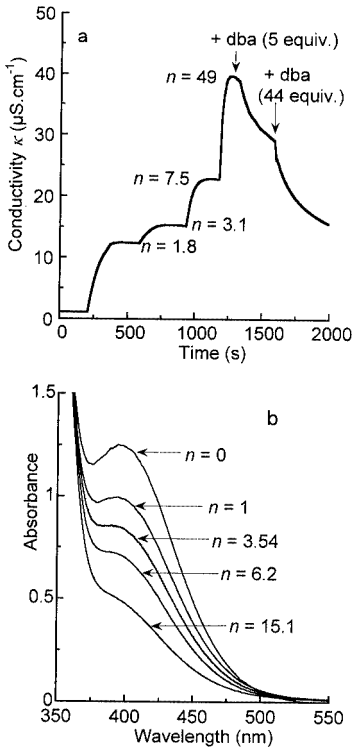

Figure 10. (a) Conductivity in DMF of the cationic complex $[(\eta^3\text{-allyl})Pd(PPh_3)_2]^+EtOCO_2^-$ (**3**) generated in the reaction of the Pd^0 complex formed from $Pd^0(dba)_2$ (2 mM) and PPh_3 (4 mM), with the cyclic allylic carbonate *cis*-**2** added successively ($0 < t < 1250$ s) (*n*: cumulative number of equiv.), followed by the successive addition of dba at 20 °C; (b) UV spectrum of $Pd^0(dba)(PPh_3)_2$, generated from $Pd^0(dba)_2$ (1 mM) and PPh_3 (2 mM) in the presence of *n* equiv. of *cis*-**2** at 20 °C, performed in DMF in a 1-mm path cell

concentration of $Pd^0(dba)(PPh_3)_2$ at different concentrations of *cis*-**2** and, thus, allowed the determination of *K*.[57]

$K = 1.4 (\pm 0.1) \times 10^{-4}$ M (DMF, 20 °C)

IV.4.2 Evidence for the Isomerization at the Allylic Position in the Oxidative Addition of Allylic Carbonate to Pd⁰ Complexes by an S_N2 Mechanism

The isomerization of *cis*-**2** to *trans*-**2** in the presence of a catalytic amount of $Pd^0(PPh_3)_4$ in THF at room temperature has been observed by Moreno-Mañas et al.[58] This reaction was reinvestigated in DMF, with $Pd^0(dba)_2$ and 2 equiv. of PPh_3, to compare the rate of isomerization as a function of the $SPd^0(PPh_3)_2$ precursor, all the while keeping in mind the fact that any oxidative addition performed from $Pd^0(PPh_3)_4$ [via $SPd^0(PPh_3)_2$] is faster than that performed from $Pd^0(dba)_2$ and 2 equiv. of PPh_3 [via $SPd^0(PPh_3)_2$] because of the higher concentration (ca. tenfold) of the reactive complex $SPd^0(PPh_3)_2$ in its equilibrium with $Pd^0(PPh_3)_3$ (Scheme 3) than in its equilibrium with $Pd^0(dba)(PPh_3)_2$ (Scheme 13).[53]

The *cis*-**2**/*trans*-**2** isomerization was observed by ^{1}H NMR spectroscopy by treating $Pd^0(dba)_2$ and 2 equiv. of PPh_3 with a stoichiometric amount of *cis*-**2** in $CDCl_3$.[57] The thermodynamic ratio (40:60)[58] was obtained after 1 h. Therefore, the reaction of the cyclic allylic carbonate *cis*-**2** with $Pd^0(dba)(PPh_3)_2$ [via $SPd^0(PPh_3)_2$] affords two cationic complexes, *cis*-**3** and *trans*-**3** (characterized by ^{31}P NMR spectroscopy), by an overall equilibrium [Equation (33)] that is established in less than 20 min, as observed by UV spectroscopy and conductivity measurements, while the overall *cis*-**2**/*trans*-**2** isomerization requires a much longer time to occur.[57]

When the same series of experiments was conducted with $Pd^0(PPh_3)_4$ in DMF, the thermodynamic ratio was reached already after 15 min. Consequently, the rate of *cis*-**2**/*trans*-**2** isomerization is faster when the precursor of $SPd^0(PPh_3)_2$ is $Pd^0(PPh_3)_4$ rather than $Pd^0(dba)_2$ and 2 equiv. of PPh_3; i.e., when the concentration of $SPd^0(PPh_3)_2$ is relatively higher. This situation supports an isomerization of the *trans*-**3** and *cis*-**3** cationic complexes proceeding through an S_N2 mechanism induced by $SPd^0(PPh_3)_2$ (Scheme 17), followed by nucleophilic attack of the ethyl carbonate anion. Thus, kinetic evidence is now available that favors the S_N2 mechanism already proposed[59a,59b] and established in the literature.[59c−59e]

One hypothesis for the *trans*-**3**/*cis*-**3** isomerization proceeding by the S_N2 mechanism is given in Scheme 18. The cationic (η^3-allyl)Pd^{II} complex *trans*-**3** would be involved in equilibrium with the cationic (η^1-allyl)Pd^{II} complex *trans*-**4**, which may be considered as an allylic derivative with the PdL_2^+ moieties as the leaving group. As classically reported for any allylic activation by a Pd^0 complex,[3] the incoming Pd^0L_2 species would first coordinate the C=C bond in an *anti* position relative to the η^1-ligated $Pd^{II}L_2^+$ moieties (complex **5**). Activation of the allylic Pd−C bond would then proceed with formation of the complex *cis*-**3** and release of Pd^0L_2, which results in an overall exchange of the $Pd^{II}L_2$ unit of the complex *trans*-**3** by the incoming Pd^0L_2 unit with inversion of the configuration to produce *cis*-**3**.

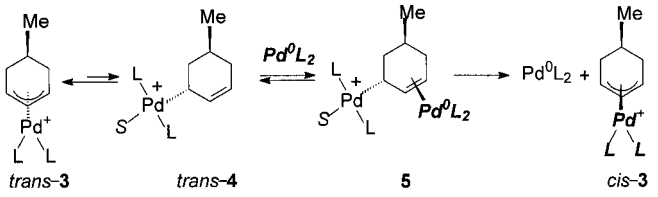

Scheme 18. Tentative explanation for the isomerization by the so-called S_N2 mechanism

It results from this mechanistic investigation that the loss of stereoselectivity in nucleophilic substitutions on the cyclic allylic carbonate *cis*-**2**, reported by Moreno-Mañas et al.,[58] arises from the isomerization of the intermediate cationic (η^3-allyl)palladium(II) complexes.

IV.5 Formation of Neutral (η^1-Allyl)(chloro)palladium Complexes in the Presence of Chloride Ions in DMF and THF

In DMF or THF, the cationic (η^3-allyl)palladium complex $[(\eta^3\text{-}CH_2CHCH_2)Pd(PPh_3)_2]^+Cl^-$ was not formed from $[Pd(\eta^3\text{-}CH_2CHCH_2)(\mu\text{-}Cl)]_2$ by addition of 4 equiv. of PPh_3 in the absence of any chloride scavenger. Indeed, the neutral complex (η^1-CH_2=$CHCH_2$)$PdCl(PPh_3)_2$ was isolated and characterized (Scheme 19).[60a] The latter complex was also generated upon addition of 1 equiv. of chloride ions (from nBu_4NCl) to the cationic $[(\eta^3\text{-}CH_2CHCH_2)Pd(PPh_3)_2]^+BF_4^-$ in DMF or THF (Scheme 19).[60a]

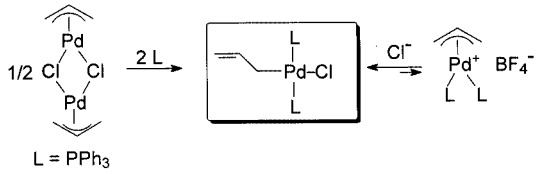

Scheme 19. Formation of (η^1-allyl)(chloro)palladium complexes

The neutral complex (η^1-CH_2=$CHCH_2$)$PdCl(PPh_3)_2$ was also generated in an oxidative addition of allyl acetate to Pd^0 complexes in the presence of voluntarily added chloride ions.[60a] This result emphasizes the crucial role of the presumably "innocent" ligands, such as chloride ions, which do not behave simply as counteranions of cationic (η^3-allyl)palladium(II) complexes, but may modify the chemical structure of the reactive intermediates by formation of neutral (η^1-allyl)(chloro)palladium(II) complexes. Consequently, the catalytic precursors of Tsuji−Trost reactions,[3] i.e., $[Pd(\eta^3\text{-}CH_2CHCH_2)(\mu\text{-}Cl)]_2$ plus 4 equiv. of PPh_3 or $[(\eta^3\text{-}CH_2CHCH_2)Pd(PPh_3)_2]^+BF_4^-$ are not equivalent. In the presence of chloride ions coming from the precursor or added in the catalytic reactions, the intermediate that is prone to react with the nucleophile might be not the cationic (η^3-allyl)palladium(II) complex, as usually considered, but the neutral (η^1-allyl)(chloro)palladium(II) species. Consequently, the presence of chloride ions might affect the regioselectivity of the catalytic reaction as well as its enantioselectivity.[61] Preliminary results on the influence of chloride ions on the reactivity of morpholine with $[(\eta^3\text{-}CH_2CHCH_2)Pd(PAr_3)_2]^+BF_4^-$ (Ar = 4-ClC_6H_4) show that the rate of nucleophilic attack is decelerated upon increasing the concentration of chloride ions. The reaction involves both cationic $[(\eta^3\text{-}CH_2CHCH_2)Pd(PAr_3)_2]^+$ and neutral (η^1-CH_2=$CHCH_2$)$PdCl(PAr_3)_2$ complexes as reactive species.[60b]

IV.6 Conclusion and Mechanistic Consequences

By means of conductivity measurements, the mechanism of the first step of the Tsuji−Trost reactions, i.e., the reaction of allylic carboxylates or carbonates with Pd^0 com-

plexes, has been more deeply established. Indeed, whether the phosphane ligand examined here is monodentate (L) or bidentate (L_2), we have used conductivity measurements to (i) characterize the cationic $[(\eta^3\text{-allyl})PdL_2]^+$ complexes formed in the reaction, with the corresponding counteranion being either carboxylates or carbonate, (ii) give evidence for the reversibility of this reaction and subsequently determined the equilibrium constants, and (iii) investigate the kinetics of formation of the cationic $[(\eta^3\text{-allyl})PdL_2]^+$ complexes.

The combination of UV spectroscopy, used to monitor the kinetics of disappearance of the Pd^0 complex, with conductivity measurements, used to monitor the kinetics of formation of the cationic complex, provides kinetic evidence that the overall reaction proceeds in two steps: first a complexation step with formation of intermediate neutral complexes $Pd^0(\eta^2\text{-}CH_2{=}CHCH_2OCOR')L_2$ ($R' = CH_3$, L_2 = dppb, dppf; $R' = Ar$, $L = PPh_3$), followed by the formation of a cationic $[(\eta^3\text{-allyl})Pd^{II}L_2]^+$ complex with $R'CO_2^-$ as the counteranion (ionization step). The better the leaving group OCOR′, the higher the concentration of the cationic complex. For good leaving groups (carbonate, trifluoroacetate), the ionization step is faster than the complexation step, whereas the ionization step is rate-determining for poorer leaving groups (acetate, benzoates).

The reaction of a cyclic allylic carbonate was found to proceed with isomerization at the allylic position when the monodentate PPh_3 ligand was considered. This finding is a consequence of the *trans*/*cis* isomerization of the cyclic $[(\eta^3\text{-allyl})Pd(PPh_3)_2]^+$ complexes by an S_N2 mechanism induced by $Pd^0(PPh_3)_2$. This mechanism, which has already been established in the literature, was confirmed kinetically by evidence that the rate of isomerization depends on the concentration of Pd^0 and its precursor. This mechanism is not restricted to cyclic allylic carbonates since we have recently observed that the reaction of a cyclic allylic benzoate also proceeds with isomerization at the allylic position, and with kinetics that are dependent on the Pd^0 precursor.[62]

This study establishes definitively that the role of the leaving group in Tsuji−Trost reactions is certainly more intricate than it is usually considered to be. Since the leaving group's concentration increases as the catalytic reaction proceeds, it may play a significant kinetic role in competing with the nucleophiles (whose concentration decreases along the catalytic reaction) in the attack on the cationic $[(\eta^3\text{-allyl})PdL_2]^+$ species. The degree of reversibility of the overall oxidative addition (which is dependent on the nature of the leaving group) controls the concentration of the available Pd^0L_2 species and, consequently, may affect the stereoselectivity of catalytic reactions performed on cyclic allylic carbonates or carboxylates by isomerization of the intermediate cyclic cationic $[(\eta^3\text{-allyl})PdL_2]^+$ complexes. The stereoselectivity may be affected also by the nature of the Pd^0 precursors, which control the concentration of available Pd^0L_2, or by the presence of chloride ions, which determine the structure of the complex reacting with the nucleophile, i.e., cationic $[(\eta^3\text{-allyl})PdL_2]^+$ or neutral $(\eta^1\text{-allyl})PdClL_2$ complexes.

V. Miscellaneous Use of Conductivity Measurements for the Investigation of the Mechanism of a Stille Reaction: Ionization of $ISnBu_3$ in DMF

When a Stille reaction is performed using an aryl iodide [Equation (34)], $ISnBu_3$ is formed quantitatively as a by-product.[7e,7f,63,64]

$$PhI + CH_2{=}CH\text{-}SnBu_3 \xrightarrow{Pd^0(dba)_2 + 2AsPh_3} Ph\text{-}CH{=}CH_2 + ISnBu_3 \quad (34)$$

Taking advantage of the fact that $ISnBu_3$ dissociates into the free ions I^- and Bu_3Sn^+ in DMF, the mechanism of the transmetallation step — reaction of $CH_2{=}CHSnBu_3$ with $PhPdI(AsPh_3)_2$ [formed in the fast oxidative addition of PhI to the Pd^0 complex generated from $Pd^0(dba)_2$ and 2 equiv. of $AsPh_3$][65] — has been investigated in DMF by conductivity measurements [Equation (35)].[66]

$$PhPdIL_2 + CH_2{=}CH\text{-}SnBu_3 \xrightarrow{DMF} Ph\text{-}CH{=}CH_2 + I^- + {}^+SnBu_3 + Pd^0L_2 \quad (35)$$
$$L = AsPh_3$$

The objective was to discriminate between the reaction of $CH_2{=}CHSnBu_3$ with $PhPdI(AsPh_3)_2$ (**6**) (Scheme 20, path **A**) or with $PhPdI(AsPh_3)(DMF)$ (**7**) (Scheme 20, path **B**), generated by the partial dissociation of $PhPdI(AsPh_3)_2$ in DMF (observed in a previous study).[65] The mechanism in path **A** has been established by Casado and Espinet for $ArPdI(AsPh_3)_2$ (Ar = C_6F_5, $C_6Cl_2F_3$) in THF,[64] whereas the mechanism in path **B** has been proposed by Farina and Krishnan for $PhPdI(AsPh_3)_2$ in THF.[63] Whatever the mechanism, the nucleophilic attack of $CH_2{=}CHSnBu_3$ gives the common complex **8**[63,64] which evolves to generate complex **9** together with I^- and Bu_3Sn^+ in DMF. Styrene is then formed by a rapid reductive elimination from **9**. Consequently, the rates of formation of styrene and of the ionic species I^- and Bu_3Sn^+ are the same and the investigation of the rate of formation of I^- and Bu_3Sn^+ by conductivity measurements will provide the rate of the overall transmetallation step and the mechanistic pathway.

In DMF, the conductivity of a solution of $PhPdI(AsPh_3)_2$ (2 mM) increased with time after addition of 10 equiv. of $CH_2{=}CHSnBu_3$ (Figure 11, a). The final conductivity was identical ($\kappa_{lim} = 76 \pm 5$ μS·cm^{-1} at 25 °C) to that measured for an authentic sample of $ISnBu_3$ (2 mM) in DMF (κ = 75 μS·cm^{-1} at 25 °C), indicating that I^- and Bu_3Sn^+ were produced quantitatively. The kinetics of formation of I^- and Bu_3Sn^+ was accelerated upon increasing the concentration of $CH_2{=}CHSnBu_3$ (reaction order of +1) and was retarded by an excess of $AsPh_3$ (Figure 11, a),[66] which is indicative of a decomplexation of the $AsPh_3$ ligand in the transmetallation step, either before of after reaction with $CH_2{=}CHSnBu_3$.

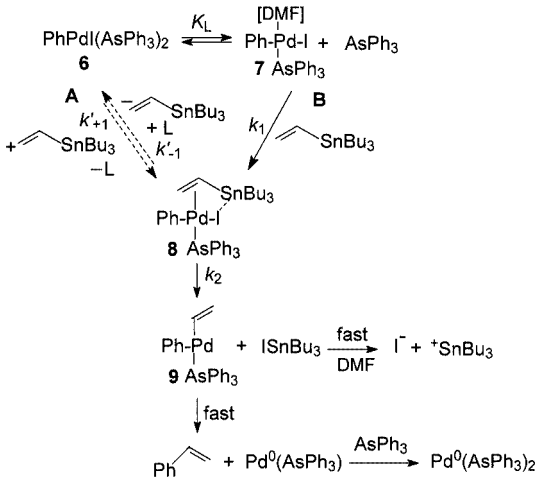

Scheme 20. Mechanism of the transmetallation step in a Stille reaction in DMF [Equation (35)]

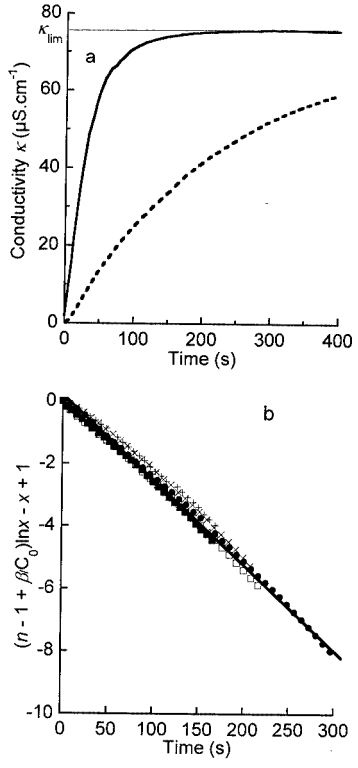

Figure 11. (a) (—) Kinetics of the reaction of CH_2=$CHSnBu_3$ (20 mM) with $PhPdI(AsPh_3)_2$ (2 mM) in DMF at 25 °C, as monitored by conductivity measurements of I^- and Bu_3Sn^+; value of $\kappa = \kappa_{exp} - \kappa_0$ (κ_{exp}: experimental conductivity at t; κ_0: initial residual conductivity of 3 $\mu S \cdot cm^{-1}$; κ_{lim}: conductivity of an authentic sample of $ISnBu_3$ (2 mM) in DMF; (---) kinetics in the presence of 5 equiv. of added $AsPh_3$; (b) influence of the concentration of $AsPh_3$ on the kinetics of the reaction of CH_2=$CHSnBu_3$ (20 mM) with $PhPdI(AsPh_3)_2$ (2 mM) in DMF at 25 °C; plot of $[(n - 1 + \beta/c_0)\ln x - x + 1]$ versus time [Equation (40)] with n = 3 (++), 4 (filled squares), 5 (empty squares), 6 (××), 7 (filled circles) [$x = (\kappa_{lim} - \kappa)/\kappa_{lim}$; κ: conductivity of I^- and Bu_3Sn^+ at t; κ_{lim}: final conductivity, determined as in Figure 11 (a)]

The kinetic laws for paths **A** and **B** (Scheme 20) are given by Equation (36) and (37), respectively (L: $AsPh_3$; Sn: CH_2=$CHSnBu_3$).[63]

$$d[I^-]/dt = d[^+SnBu_3]/dt = -d[\mathbf{6}]/dt = \frac{k'_{+1}k_2[\mathbf{6}][Sn]([L] + K_L)}{(k'_{-1}[L] + k_2)[L]} \quad (36)$$

$$d[I^-]/dt = d[^+SnBu_3]/dt = -d[\mathbf{6}]/dt = \frac{k_1K_L[\mathbf{6}][Sn]}{[L] + K_L} \quad (37)$$

Taking into account the value of $K_L = 3.1 \times 10^{-4}$ M in DMF,[65] Equation (36) simplifies into Equation (38) at high concentrations of L ([L] > 6 mM) so that paths **A** and **B** could not be distinguished on the basis of the observed rate law at high concentrations of L. Both laws can be expressed as Equation (39) with $\alpha = k_1 \cdot K_L$ and $\beta = K_L$ for Equation (37) and $\alpha = k_2 \cdot K'_1$ and $\beta = k_2/k'_{-1}$ for Equation (38).

$$-d[\mathbf{6}]/dt = \frac{k_2K'_1[\mathbf{6}][Sn]}{[L] + k_2/k'_{-1}} \quad (38)$$

$$-d[\mathbf{6}]/dt = \frac{\alpha[\mathbf{6}][Sn]}{[L] + \beta} \quad (39)$$

Because of the limiting solubility of $AsPh_3$ in DMF (14 mM), $AsPh_3$ could not be added in large excess. Therefore, the concentration of $AsPh_3$ was not constant during the reaction and the integration of Equation (39) gives Equation (40) with $x = (\kappa_{lim} - \kappa)/\kappa_{lim}$ (determined as in Figure 11, a) and n being the initial number of equiv. of $AsPh_3$ added to $Pd^0(dba)_2$ before addition of 1 equiv. of PhI, which generates $PhPdI(AsPh_3)_2$.

$$(n - 1 + \beta/C_0)\ln x - x + 1 = -\frac{\alpha[Sn]t}{C_0} \quad (40)$$

A value of $\beta = 3.2 \times 10^{-4}$ was determined, so that the plot of $(n - 1 + \beta/c_0)\ln x - x + 1$ versus time was linear whatever the value of n (Figure 11, b) in agreement with Equation (40), which is then valid over the whole range of concentrations of $AsPh_3$ added to $PhPdI(AsPh_3)_2$ (2–10 mM). Consequently, the experimental kinetics of the transmetallation step are in agreement with the mechanism of path **B** in Scheme 20; this conclusion would not be the case for the mechanism of path **A**, since Equation (38) is valid only for high concentrations of $AsPh_3$ (> 6 mM). Since $\beta = K_L$ [Equations (37) and (39)], a second method to determine $K_L = 3.2 \pm 0.1 \times 10^{-4}$ M (DMF, 25 °C) is available and is in agreement with the value of $K_L = 3.1 \times 10^{-4}$ M (DMF, 25 °C) determined in a previous study.[65]

Since $\alpha = k_1 \cdot K_L$, then $k_1 = 8.3 \pm 0.5$ $M^{-1}s^{-1}$. A similar value of $k_1 = 7.5$ $M^{-1}s^{-1}$(DMF, 25 °C) was determined by treating CH_2=$CHSnBu_3$ with $PhPdI(AsPh_3)$(DMF) generated by the fast dissociation of the dimer $Ph_2Pd_2(\mu\text{-}I)_2(AsPh_3)_2$ (**10**) in DMF.[66] The kinetics of this system were also monitored by conductivity measurements of I^- and Bu_3Sn^+ generated in the reaction.[66]

Therefore, K_L has been determined independently by two different strategies: (i) from the partial dissociation of

$PhPdI(AsPh_3)_2$ to $PhPdI(AsPh_3)(DMF)$ observed in DMF,[65] and (ii) from the kinetics of the transmetallation step performed with $PhPdI(AsPh_3)_2$ [66] (vide supra). Similarly, the same value of k_1, which characterizes the reactivity of $PhPdI(AsPh_3)(DMF)$ with $CH_2{=}CHSnBu_3$, has been determined independently by two different strategies: (i) from the kinetics of the transmetallation step performed with $PhPdI(AsPh_3)_2$ (vide supra)[66] and (ii) from the kinetics of the reaction of $CH_2{=}CHSnBu_3$ with $PhPdI(AsPh_3)(DMF)$ generated by the fast dissociation of the dimer **10** in DMF.[66]

This result definitively proves that, in DMF, the transmetallation step involves the reaction of $CH_2{=}CHSnBu_3$ with $PhPdI(AsPh_3)(DMF)$ generated by dissociation of $PhPdI(AsPh_3)_2$ (path **B** in Scheme 20). This study illustrates how to take advantage of conductivity measurements, used to monitor the kinetics of the formation of a by-product, to gain a deeper insight into the mechanism of a palladium-catalyzed reaction that does not involve any ionic palladium complexes as intermediates.

Conclusion

Taking advantage of the fact that DMF is a good solvent for dissociating and coordinating cationic palladium(II) complexes, conductivity measurements have proved to be efficient for characterizing the cationic nature of palladium(II) complexes that have already been postulated in the literature, but not characterized in the context of a real oxidative addition, such as (i) $[(aryl)PdL_2(DMF)]^+TfO^-$ or $[(vinyl)PdL_2(DMF)]^+TfO^-$ ($L = PPh_3$) generated in oxidative additions of aryl or vinyl triflates, respectively, to Pd^0 complexes, (ii) $[HPdL_2(DMF)]^+RCO_2^-$ ($R = CH_3$, H; $L = PPh_3$) generated in oxidative additions of acetic or formic acid to Pd^0 complexes, and (iii) $[(\eta^3\text{-allyl})PdL_2]^+R'CO_2^-$ (R' = alkyl, aryl, OEt; $L = PPh_3$ or L_2 = dppe, dppf) in oxidative additions of allylic carboxylates (or carbonates) to Pd^0 complexes. In all cases, the cationic palladium(II) complex and its counteranion were generated as free ions. Such cationic complexes are key intermediates in Stille, Heck, and Tsuji–Trost reactions. The role of chloride ions has been investigated with the formation of neutral complexes $ArPdClL_2$ and $(\eta^1\text{-allyl})PdClL_2$ ($L = PPh_3$). The cationic and neutral character of the intermediate Pd^{II} complexes is of crucial importance because it determines their reactivities with nucleophiles in Heck, Stille, and Tsuji–Trost reactions.

Conductivity measurements have also been used to gather thermodynamic data on the formation of cationic palladium(II) complexes. Indeed, the reversibility of oxidative additions of allylic carboxylates (or carbonates) to Pd^0 complexes has been established as well as that of acetic and formic acid, and the equilibrium constants have been determined. The reversible oxidative addition of a cyclic allylic carbonate generates cyclic *cis* and *trans* $[(\eta^3\text{-allyl})PdL_2]^+EtOCO_2^-$ complexes. The *cis*/*trans* isomerization proceeds by an S_N2 mechanism induced by the Pd^0L_2 complex.

Conductivity measurements have also been used to gather kinetic data on the formation of cationic palladium(II) complexes. Under conditions where the oxidative additions were irreversible, the rates of formation of the cationic palladium(II) complexes (monitored by conductivity measurements) were compared to those of the disappearance of the palladium(0) complex (monitored by UV spectroscopy). Kinetic evidence has been obtained for the formation of neutral intermediate complexes $Pd^0(\eta^2\text{-allyl-OCOR}')L_2$ ($R' = CH_3$, L_2 = dppb, dppf; $R' = Ar$, $L = PPh_3$) in the oxidative addition of allylic carboxylates to palladium(0) complexes, establishing that two successive reactions are involved (complexation and ionization steps) whose relative rates depend on the nature of the leaving group $-OCOR'$. Thus, the effect of the leaving group has been clarified.

As a somewhat unrelated application of this method, monitoring the formation of an ionic by-product (I^-, $^+SnBu_3$) by conductivity measurements has brought about a deeper insight into the mechanism of the transmetallation step of a Stille reaction, which does not involve any ionic intermediate palladium complexes, by establishing the involvement of $PhPdI(AsPh_3)(DMF)$ as the species that reacts with an organotin derivative.

Acknowledgments

The author wishes to express her gratitude to the students who have greatly contributed to the research work summarized here: S. Gamez, A. Mosleh, A. Ndedi Ntepe, C. Orthwein as well as Dr. G. Meyer and Prof. C. Amatore. Drs. I. Chiarotto, K. K. Hii, R. Pleixats, Profs. J. B. Brown, I. Carelli, M. Moreno-Mañas and J. G. de Vrieze are thanked for fruitful collaborations. S. Négri is also thanked for technical assistance. The financial support from CNRS, ENS (MNRT) and University Paris VI is gratefully acknowledged. Johnson Matthey is thanked for a generous loan of sodium tetrachloropalladate.

[1] [1a] A. de Mejeire, F. E. Meyer, *Angew. Chem. Int. Ed. Engl.* **1994**, *33*, 2379–2411. [1b] G. T. Crisp, *Chem. Soc., Rev.* **1998**, *27*, 427–436. [1c] I. P. Beletskata, A. V. Cheprakov, *Chem. Rev.* **2000**, *100*, 3009–3066. [1d] M. Larhed, A. Hallberg, *Handbook of Organopalladium Chemistry for Organic Synthesis* (Ed.: E. Negishi), Wiley-Interscience, New York, **2002**, vol. I, chapter IV.2, p. 1133–1178.

[2] For Heck reactions from aryl triflates, see: [2a] W. Cabri, I. Candiani, S. DeBernardinis, F. Francalanci, S. Penco, R. Santi, *J. Org. Chem.* **1991**, *56*, 5796–5800. [2b] F. Ozawa, A. Kubo, T. Hayashi, *J. Am. Chem. Soc.* **1991**, *113*, 1417–1419. [2c] T. Hayashi, A. Kubo, F. Ozawa, *Pure Appl. Chem.* **1992**, *64*, 421–427. [2d] W. Cabri, I. Candini, A. Bedeschi, R. Santi, *J. Org. Chem.* **1992**, *57*, 3558–3563. [2e] F. Ozawa, A. Kubo, Y. Matsumoto, T. Hayashi, *Organometallics* **1993**, *12*, 4188–4196. [2f] W. Cabri, I. Candini, *Acc. Chem. Res.* **1995**, *28*, 2–7.

[3] [3a] J. Tsuji, *Palladium Reagents and Catalysts*, John Wiley & Sons, Chichester, **1996**, p. 290. [3b] S. A. Godleski, in *Comprehensive Organic Synthesis*, vol. 4 (Eds: B. M. Trost, I. Flemming, M. F. Semmelhack), Pergamon, Oxford, **1991**. [3c]G. Consiglio, R. Waymouth, *Chem. Rev.* **1989**, *89*, 257–276. [3d] C. G. Frost, J. Howard, J. M. J. Williams, *Tetrahedron: Asymmetry* **1992**, *3*, 1089–1122. [3e] A. Pfaltz, *Acc, Chem. Rev.* **1993**, *26*, 339–345. [3f] B. M. Trost, *Acc. Chem. Res.* **1996**, *29*, 355–364. [3g] B. M. Trost, D. L. Van Kanken, *Chem. Rev.* **1996**, *96*, 395–422.

[4] P. W. Atkins, *Physical Chemistry*, 5th ed., Oxford University Press, **1994**, p. 834−839.

[5] Modern conductivity meters (e.g., CDM210 Radiometer Analytical) deliver the conductivity κ of solutions containing ionic species. $\kappa = kG$ where G is the conductance ($G = 1/R$; R: resistance of the solution containing the ionic species) expressed in Siemens (S; 1 S = 1 Ω^{-1}) and k is the cell constant expressed in cm^{-1} (the value of k is usually close to 1 cm^{-1}). The measured conductivity κ is expressed in $S{\cdot}cm^{-1}$. Considering a strong electrolyte with c_i being the concentration of one ion, z_i its charge and λ_i its equivalent conductivity, the overall conductivity is expressed as $\kappa = \Sigma\lambda_i z_i c_i$ if the solution behaves ideally. In the case of a 1:1 electrolyte at a concentration c, $\kappa = (\lambda_+ + \lambda_-)c = \Lambda_M c$. The molar conductivity Λ_M of the electrolyte is usually expressed in $S{\cdot}cm^2{\cdot}mol^{-1}$ when the concentration C is expressed in $mol{\cdot}L^{-1}$.[4] The conductivity can be recorded versus time using a computerized home-made program.

[6] For a review on the characterization of coordination compounds by conductivity measurements, see: W. J. Geary, *Coord. Chem. Rev.* **1971**, *7*, 81−122.

[7] [7a] W. J. Scott, G. T. Crisp, J. K. Stille, *J. Am. Chem. Soc.* **1984**, *106*, 4630−4632. [7b] W. J. Scott, J. K. Stille, *J. Am. Chem. Soc.* **1986**, *108*, 3033−3040. [7c] A. M. Echavarren, J. K. Stille, *J. Am. Chem. Soc.* **1987**, *109*, 5478−5486. [7d] A. M. Echavarren, J. K. Stille, *J. Am. Chem. Soc.* **1988**, *110*, 1557−1565. [7e] V. Farina, G. P. Roth, *Adv. Metalorg. Chem.* **1996**, *5*, 1−53. [7f] V. Farina, V. Krishnamurthy, W. J. Scott, *Org. React.* **1997**, *50*, 1−339.

[8] P. J. Stang, M. H. Kowalski, M. D. Schiavelli, D. Longford, *J. Am. Chem. Soc.* **1989**, *111*, 3347−3356.

[9] V. Farina, B. Krishnan, D. R. Marshall, G. P. Roth, *J. Org. Chem.* **1993**, *58*, 5434−5444.

[10] A. Jutand, A. Mosleh, *Organometallics* **1995**, *14*, 1810−1817.

[11] The oxidative addition of 4-$O_2NC_6H_4OTf$ to $Pd^0(PPh_3)_4$ in THF was monitored by ^{31}P NMR spectroscopy at room temperature. The spectrum exhibits a singlet at δ = 22.2 ppm attesting that only *trans*-[4-$O_2NC_6H_4Pd(PPh_3)_2(THF)]^+TfO^-$ was formed and not [4-$O_2NC_6H_4Pd(PPh_3)_3]^+TfO^-$. Espinet et al. have reported that $[C_6F_5Pd(PPh_3)_3]^+TfO^-$ was generated as a minor complex in the oxidative addition of C_6F_5OTf to $Pd^0(PPh_3)_4$ in THF at 20 °C.[12]

[12] A. L. Casado, P. Espinet, A. M. Gallego, *J. Am. Chem. Soc.* **2000**, *122*, 11771−11782.

[13] Espinet et al. have reported that a related neutral complex *trans*-$(C_6Cl_2F_3)Pd(OTf)(PPh_3)_2$ predominates in the equilibrium with the ionic *trans*-$[(C_6Cl_2F_3)Pd(PPh_3)_2(THF)]^+$ and TfO^- at low temperatures in THF, but had almost disappeared above room temperature. The cationic complex was then predominant.[12]

[14] C. Amatore, M. Azzabi, A. Jutand, *J. Am. Chem. Soc.* **1991**, *113*, 8375−8384.

[15] A. Jutand, A. Mosleh, *J. Org. Chem.* **1997**, *62*, 261−274.

[16] [16a] C. Amatore, A. Jutand, M. A. M'Barki, *Organometallics* **1992**, *11*, 3009−3013. [16b] C. Amatore, E. Carré, A. Jutand, M. A. M'Barki, G. Meyer, *Organometallics* **1995**, *14*, 5605−5614. [16c] C. Amatore, A. Jutand, *Acc. Chem. Res.* **2000**, *33*, 314−321.

[17] A. Jutand, K. K. Hii, M. Thornton-Pett, J. M. Brown, *Organometallics* **1999**, *18*, 5367−5374.

[18] L. M. Alcazar-Roman, J. F. Hartwig, *Organometallics* **2002**, *21*, 491−502.

[19] A. L. Casado, P. Espinet, A. M. Gallego, J. M. Martínez-Ilarduya, *Chem. Commun.* **2001**, 339−340.

[20] [20a] J. M. Brown, J. J. Pérez-Torrente, N. W. Alcock, H. J. Clase, *Organometallics* **1995**, *14*, 207−213. [20b] J. M. Brown, K. K. Hii, *Angew. Chem. Int. Ed. Engl.* **1996**, *35*, 657−659.

[21] M. Ludwig, S. Strömberg, M. Svensson, B. Åkermark, *Organometallics* **1999**, *18*, 970−975.

[22] J. F. Fauvarque, F. Pflüger, M. Troupel, *J. Organomet. Chem.* **1981**, *208*, 419−427.

[23] B. E. Mann, A. Musco, *J. Chem. Soc., Dalton Trans.* **1968**, *14*, 5605−5614.

[24] C. Amatore, E. Carré, A. Jutand, *Acta Chem. Scand.* **1998**, *52*, 100−106.

[25] K. K. Hii, M. Thornton-Pett, A. Jutand, R. P. Tooze, *Organometallics* **1999**, *18*, 1887−1896.

[26] [26a] K. Karabelas, C. Westerlund, A. Hallberg, *J. Org. Chem.* **1985**, *50*, 3896−3900. [26b] W. Cabri, I. Candiani, A. Bedeshi, R. Santi, *Tetrahedron Lett.* **1991**, *32*, 1753−1756.

[27] [27a] R. J. Deeth, A. Smith, K. K. Hii, J. M. Brown, *Tetrahedron Lett.* **1998**, *39*, 3229−3232. [27b] K. K. Hii, T. D. W. Claridge, J. M. Brown, *Angew. Chem. Int. Ed. Engl.* **1997**, *36*, 984−987.

[28] L. E. Overman, D. J. Poon, *Angew. Chem. Int. Ed. Engl.* **1997**, *36*, 518−521.

[29] A. Jutand, S. Négri, submitted.

[30] [30a] T. Sakamoto, Y. Kondo, N. Mutura, H. Yamanaka, *Tetrahedron* **1993**, *49*, 9713−9720. [30b] R. Kakino, S. Yasumi, I. Shimizu, A. Yamamoto, *Bull. Chem. Soc. Jpn.* **2002**, *75*, 137−148.

[31] M. S. Stephan, A. J. J. M. Teunissen, G. K. M. Verzijl, J. G. de Vries, *Angew. Chem. Int. Ed.* **1998**, *37*, 662−664.

[32] A. Jutand, S. Négri, J. G. de Vries, *Eur. J. Inorg. Chem.* **2002**, 1711−1717.

[33] [33a] B. M. Trost, W. Pfrengle, H. Urabe, J. Dumas, *Acc. Chem. Res.* **1990**, *23*, 34−42. [33b] B. M. Trost, M. J. Krische, *Synlett* **1998**, 1−16. [33c] B. M. Trost, *Chem. Eur. J.* **1998**, *4*, 2405−2412.

[34] D. Zargarian, H. Alper, *Organometallics* **1993**, *12*, 712−724.

[35] I. Carelli, I. Chiarotto, S. Cacchi, P. Pace, C. Amatore, A. Jutand, G. Meyer, *Eur. J. Org. Chem.* **1999**, 1471−1473.

[36] For a review on hydrido complexes of palladium, see: V. V. Grushin, *Chem. Rev.* **1996**, *96*, 2011−2033.

[37] C. Amatore, A. Jutand, G. Meyer, I. Carelli, I. Chiarotto, *Eur. J. Inorg. Chem.* **2000**, 1855−1859.

[38] A. R. Siedle, R. A. Newmark, W. B. Gleason, *Inorg. Chem.* **1991**, *30*, 2005−2009.

[39] V. N. Zudin, V. D. Chinakov, V. M. Nekipelov, V. A. Likholobov, Y. I. Yermakov, *J. Organomet. Chem.* **1985**, *289*, 425−430.

[40] The conductivity did not stabilize, but instead it increased continually with time at 25 °C. The degradation probably arose from a side reaction induced by the formate ion, i.e., the partial decarboxylation of the neutral intermediate HPd(OCHO)$(PPh_3)_2$ (formed in the very first step of the reaction) before ionization. This well-known decarboxylation of formate gave $HPdH(PPh_3)_2$, leading to H_2 and Pd^0L_2 that again underwent a reaction with HCO_2H. A similar degradation has been proposed by Zargarian and Alper.[34]

[41] If, however, the catalytic reactions are carried out in benzene, a non-coordinating and non-ionizing solvent, the neutral complexes $HPdA(PPh_3)_2$ (A = $OCOCH_3$ or OCHO)[33a,33b] must be formed, but in low concentration because they are involved in an endergonic equilibrium with the carboxylic acid and the Pd^0 complex.

[42] J. Tsuji, *Tetrahedron* **1986**, *42*, 4361−4401.

[43] Few cationic (η^3-allyl)palladium(II) complexes formed by an oxidative addition of an allylic acetate have been reported with acetate as the counter anion. See: [43a] T. Yamamoto, O. Saito, A. Yamamoto, *J. Am. Chem. Soc.* **1981**, *103*, 5600−5602. [43b] P. R. Auburn, P. B. Mackenzie, B. Bosnich, *J. Am. Chem. Soc.* **1985**, *107*, 2033−2046. [43c] A cationic (η^3-allyl)palladium(II) complex has been synthesized by oxidative addition of an allylic acetate to a Pd^0 complex, but with BF_4^- as the counteranion because of treatment of the complex with $NaBF_4$ before isolation. See: T. Hayashi, T. Hagihara, M. Konishi, M. Kumada, *J. Am. Chem. Soc.* **1983**, *105*, 7767−7768. [43d] T. Hayashi, A. Yamamoto, T. Hagihara, *J. Org. Chem.* **1986**, *51*, 723−727.

[44] [44a] J. Powell, B. L. Shaw, *J. Chem. Soc. A* **1968**, 774−777. [44b] B. Åkermark, G. Åkermark, L. S. Hegedus, K. Zetterberg, *J. Am. Chem. Soc.* **1981**, *103*, 3037−3040.

[45] T. Hayashi, A. Yamamoto, Y. Ito, E. Nishioka, H. Miura, K. Yanagi, *J. Am. Chem. Soc.* **1989**, *111*, 6301−6311.

[46] C. Amatore, A. Jutand, G. Meyer, L. Mottier, *Chem. Eur. J.* **1999**, *5*, 466−473.
[47] C. Amatore, S. Gamez, A. Jutand, *Chem. Eur. J.* **2001**, *7*, 1273−1280.
[48] C. Amatore, S. Gamez, A. Jutand, *J. Organomet. Chem.* **2001**, *624*, 217−222.
[49] C. Amatore, S. Gamez, A. Jutand, G. Meyer, L. Mottier, *Electrochim. Acta* **2001**, *46*, 3237−3244.
[50] N. Agenet, C. Amatore, S. Gamez, H. Gérardin, A. Jutand, G. Meyer, C. Orthwein, *ARKIVOC* **2002**, 92−101 (http://www.arkat-usa.org/).
[51] For seminal works on the use of $Pd(dba)_2$ with monodentate phosphane ligands in allylic substitutions, see: D. Ferroud, J. P. Genêt, J. Muzart, *Tetrahedron Lett.* **1984**, *25*, 4379−4382.
[52] For seminal works on the use of $Pd(dba)_2$ with bidentate phosphane ligands in allylic substitutions, see: J. C. Fiaud, H. de Gournay, M. Larchevêque, H. B. Kagan, *J. Organomet. Chem.* **1978**, *154*, 175−185.
[53] [53a] C. Amatore, A. Jutand, F. Khalil, M. A. M'Barki, L. Mottier, *Organometallics* **1993**, *12*, 3168−3178. [53b] C. Amatore, A. Jutand, *Coord. Chem. Rev.* **1998**, *178−180*, 511−528.
[54] [54a] B. M. Trost, T. R. Verhoeven, J. F. Fortunak, S. M. McElvain, *Tetrahedron Lett.* **1979**, *25*, 2301−2304. [54b] B. M. Trost, T. R. Verhoeven, *J. Am. Chem. Soc.* **1980**, *102*, 4730−4743. [54c] J.-E. Bäckvall, R. E. Nordberg, J. Vagberg, *Tetrahedron Lett.* **1983**, *24*, 411−412.
[55] C. Amatore, G. Broeker, A. Jutand, F. Khalil, *J. Am. Chem. Soc.* **1997**, *119*, 5176−5185.
[56] For stable cationic complexes $[(\eta^3\text{-allyl})PdL_2]^+$ (L = PMe_3, PMe_2Ph, $PMePh_2$) with ethyl carbonate as the counteranion, see: F. Ozawa, T. Son, S. Ebina, K. Osakada, A. Yamamoto, *Organometallics* **1992**, *11*, 171−176.
[57] C. Amatore, S. Gamez, A. Jutand, G. Meyer, M. Moreno-Mañas, L. Morral, R. Pleixats, *Chem. Eur. J.* **2000**, *6*, 3372−3376.
[58] M. Moreno-Mañas, L. Morral, R. Pleixats, *J. Org. Chem.* **1998**, *63*, 6160−6166.
[59] [59a] T. Takahashi, Y. Jinbo, K. Kitamura, J. Tsuji, *Tetrahedron Lett.* **1984**, *25*, 5921−5924. [59b] P. B. Mackenzie, J. Whelan, B. Bosnich, *J. Am. Chem. Soc.* **1985**, *107*, 2046−2054. [59c] H. Kurosawa, S. Ogoshi, N. Chatani, Y. Kawasaki, S. Murai, I. Ikeda, *Chem. Lett.* **1990**, 1745−1748. [59d] J-E. Bäckvall, K. L. Granberg, A. Heumann, *Isr. J. Chem.* **1991**, *31*, 17−24. [59e] K. L. Granberg, J.-E. Bäckvall, *J. Am. Chem. Soc.* **1992**, *114*, 6858−6863.
[60] [60a] C. Amatore, A. Jutand, M. A. M'Barki, G. Meyer, L. Mottier, *Eur. J. Inorg. Chem.* **2001**, 873−880. [60b] T. Cantat, A. Jutand, G. Meyer, submitted.
[61] [61a] G. C. Lloyd-Jones, S. C. Stephen, *Chem. Commun.* **1998**, 2321−2322. [61b] G. C. Lloyd-Jones, S. C. Stephen, *Chem. Eur. J.* **1998**, *4*, 2539−2549. [61c] B. M. Trost, F. D. Toste, *J. Am. Chem. Soc.* **1999**, *121*, 4545−4555.
[62] C. Amatore, J. C. Fiaud, A. Jutand, L. Mensah, G. Meyer, unpublished results.
[63] V. Farina, B. Krisnan, *J. Am. Chem. Soc.* **1991**, *113*, 9585−9595.
[64] A. L. Casado, P. Espinet, *J. Am. Chem. Soc.* **1998**, *120*, 8978−8985.
[65] C. Amatore, A. Bucaille, A. Fuxa, A. Jutand, G. Meyer, A. Ndedi Ntepe, *Chem. Eur. J.* **2001**, 2134−2142.
[66] C. Amatore, A. Bahsoun, A. Jutand, G. Meyer, A. Ndedi Ntepe, L. Ricard, *J. Am. Chem. Soc.*, **2003**, *115*, 4212−4222.

Received February 4, 2003

